

– unless any members of your groups are included in the “*et al*”, you must fax/email us a letter of permission from this group – or delete from text.) In the second phase, the accumulation of GPI and anti-GPI may reflect deposits of the complexes circulating in serum; the increased vascular permeability now allows better entry of complexes and, by then, all circulating GPI is complexed by the large excess of antibodies present. (AUTHOR – rephrasing in last para OK?)

RA is a multifaceted disease and the model described here certainly represents a simplification of the mechanisms that could contribute to the variety of arthritic conditions in humans. Additional pathways and mechanisms, such as secondary immune responses to joint structures or indirect consequences of the synovial hyperproliferation, must contribute to the complex events of established RA. The model proposed above also has many conceptual precedents, in particular in the ideas of immune complex pathology that were prevalent in the early 1970s<sup>29,30</sup>. In essence, this view of arthritis is a form of type III hypersensitivity (Arthus) reaction, which is localized to the joint. In focusing attention on specific molecules and effector pathways, the K/BxN mouse does, however, provide a focal point around which to synthesize this view of the early stages of arthritogenesis. (AUTHOR – rephrasing in last para OK?)

Finally, the serum GPI concentrations followed an unexpected pattern: they dropped markedly during the first weeks of age. This may reflect a fetal or early neonatal cellular release of the enzyme, perhaps related to the extensive tissue proliferation and growth that occurs during this period or to fetomaternal interactions. In any case, the pattern likely explains the development of T cell tolerance observed in K/BxN mice: It was complete during the first weeks of age, showed strong clonal deletion in the thymus and was less stringent later on, so that clonotype-positive reactive cells matured in the peripheral organs and were only partially anergized. It will be important to determine whether this pattern is involved in establishing imperfect tolerance and is a general feature of self-antigens that are involved in certain forms of arthritis. (AUTHOR – rephrasing in last para OK?)

The KRN model of arthritis, although very different in its immunological phase, dovetails with the classical arthritis model induced by collagen II immunization, in which IgG binds to the cartilage surface. This shows how different pathogenic mechanisms and autoimmune targets may converge to a common effector pathway in human arthritic diseases. (AUTHOR – rephrasing in last para OK?)

## Methods

**Mice and arthritis.** K/BxN TCR-Tg mice were as described<sup>1</sup>. They were maintained by serial crossing onto the B10.BR genetic background and, as such, were asymptomatic. Arthritic offspring were produced by crossing to the NOD/Li strain. Recombination-activating gene 1-deficient mice were a gift of F. Alt (Children's Hospital, Boston). B6 mice were from the Jackson Laboratory (Bar Harbor, ME). Arthritis was spontaneous in K/BxN mice or was induced in normal inbred mice by injection of 2x150 µl of K/BxN serum. For fractionation, K/BxN and control BxN sera (2–3 ml) were separated by size-exclusion chromatography with a Superdex 200 column (Amersham Pharmacia Biotech, Piscataway, NJ). Fractions (4 ml) were collected, pooled and concentrated before ELISA analysis of injection into mice. (AUTHOR – rephrasing OK?)

**RNA analysis.** RNA was prepared from kidney tissue by a modified LiCl-Urea technique<sup>31</sup>. After dissection of ankles (sectioned at the long bones of the lower leg and in the metatarsal area), the skin and superficial tendons were removed and the remaining tissue was immersed in 1 ml of RNA solubilization solution (without LiCl). Articular cavities were opened with a scalpel and were dissected in the medium to release the cellular contents. Concentrated LiCl solution (6 M LiCl, 6 M urea and 10 mM Na acetate at pH 5) was then added to precipitate the RNA. cDNA was synthesized from these RNAs by MuLV reverse transcriptase (Gibco-BRL, Gaithersburg, PA).

To search for alternative forms within the coding region, PCR primers were used to amplify the coding sequence (Fig. 1a, pair 1; all primer sequences available on request. AUTHOR – you must provide the actual sequences, pls email them to us as a Word doc. This is a condition of publication – Editor), the products were cloned into PCR2.1 vector and three independent plasmids were sequenced (ABI 373A (AUTHOR – is this a

Genbank #? If yes, please specify what this # relates to)) with internal primers (Fig. 1a). For RACE analysis of mRNA termini, the protocol was as described<sup>32</sup>. For the 3' end, the mRNA was reverse-transcribed with a dT-adaptor primer (R3'). A 10 µl aliquot was used for 40 cycles of PCR (at the same temperatures used above. AUTHOR – above where?) with the adaptor primer and sense primer R3. The reaction products were separated by agarose gel electrophoresis, blotted and detected with a labeled PCR product that covered the 3' end of the GPI coding region. These RACE products were also sequenced. For quantitative real-time analysis, PCR was done on a TaqMan PRISM 7700 instrument (PE Applied Biosystems, Foster City, CA), and data was analyzed with the instrument software. Amplification was done in triplicate in 96-well plates using intron-spanning specific primers and the antisense fluorogenic probe labeled with a 5' 6-carboxy-fluorescein (FAM) reporter dye and a 3' 6-carboxy-tetramethyl-rhodamine (TAMRA) quencher (sense primer 5'-AGATCAACTACACCGAGGATCG-3'; antisense primer 5'-ACATCTTTGCCGTC-CACCTT-3'; probe 5'-FAM-TGCCCTTCGGAAACCGGTCC-TAMRA-3'). A cyclophilin primer combination was used as a standard. (AUTHOR – rephrasing OK?)

**Immunoblot and protein analysis.** For immunoblotting, ankles and kidney (two of each) were minced and the contents extracted in 500 µl of lysis solution (50 mM Tris-HCl at pH 7.4, 5 mM MgCl<sub>2</sub>, 0.5% NP40 and 2 mM PMSF). Whole lysate (15 µg) was separated by PAGE and blotted into PVDF membranes (Bio-Rad, Hercules, CA). After blocking with 5% milk in PBS, K/BxN serum (1/1000) or mouse anti-actin (Sigma, St. Louis, MO) was used as a probe. Bound antibody was detected with horseradish peroxidase (HRP)-conjugated goat anti-mouse IgG (Jackson ImmunoResearch, West Grove, PA) using a Super-Signal kit (Pierce, Rockford, IL) and chemiluminescence was imaged quantitatively. For 2D immunoblotting, kidney or ankle extracts (10 µg) or a 1/1 mixture were diluted in sample buffer (40 µl, 9.5 M urea, 2% NP40, 2% ampholines at pH 3.5–10 and 5% β-mercaptoethanol) and were loaded onto a first-dimension tube gel (9.5 M urea, 3.35% acrylamide, 2% NP40 and 2% ampholines at pH 3.5–10). After electrophoresis, the tube gels were loaded onto a 10% acrylamide slab gel and GPI was detected as above. (AUTHOR – rephrasing OK?)

**Immunohistology.** For immunohistology, cryostat sections from ankle joints were prepared with the tape-capture technique as described<sup>33</sup>. Anti-GPI polyclonal Igs were affinity-purified from K/BxN serum as described<sup>1</sup>; protein G-purified IgG from normal BxN mice was used as a control. Igs were conjugated to FITC (Fluorescein-EX, Molecular Probes, Eugene, OR) according to the manufacturer's instructions. Other reagents were Texas red-conjugated anti-mouse IgG (Jackson), and FITC-conjugated goat anti-mouse C3 (ICN Biomedicals, Costa Mesa, CA). After blocking with 2% bovine serum albumin and 0.04% Tween in PBS, the sections were stained with anti-GPI or control Ig (500 ng/section). Nuclei were counterstained with DAPI (50 ng/section, Molecular Probes). Fluorescence was detected on a conventional Zeiss Axioplan2 microscope or by confocal microscopy (LSM 410 confocal microscope, with 364, 488 or 568 nm excitation, Zeiss, Thornwood, NY). Images were acquired and processed digitally (Photoshop 6.0). (AUTHOR – rephrasing OK?)

**ELISA assays.** Antibodies to GPI were detected as described<sup>1</sup>. To quantify GPI in serum, a sandwich ELISA assay was developed with a recently isolated GPI mAb (M. M., unpublished data). Anti-GPI (mAb 6.121, 10 µg/ml) was used to coat a microtiter plate, and test serum (1/100) was added and incubated for 2 h at room temperature. After washing, biotinylated (Fluorescein-biotin-dinitrophenol, Molecular Probes) polyclonal anti-GPI Ig, which was affinity-purified from K/BxN serum, was added to the plate (1/1000). The plate was incubated for 1 h and was detected with allophycocyanin-streptavidin (Jackson ImmunoResearch); all incubations were done at room temperature. Recombinant mouse GPI<sup>1</sup> was used as a standard. To detect immune complexes, ELISA plates (Maxisorb, Nunc, Roskilde, Denmark) were coated with 20 µg/ml of C1q (Sigma) in PBS at 4 °C overnight, blocked with bovine serum albumin before incubation with serum dilutions and bound complexes were detected with phosphatase-coupled anti-mouse IgG (Jackson ImmunoResearch). (AUTHOR – rephrasing OK?)

## Acknowledgments

We thank J. L. Pasquali for enlightening discussions; J. Hergueux, S. Johnson and Q. M. Pham for managing the KRN colony; C. Cahill for help with confocal microscopy; P. Gerber for ELISAs and chromatography; and D. Bowman and A. Calderone for sections. Supported by institutional funds from the INSERM, CNRS and the Centre Hospitalo-Universitaire and by grants from the Association pour la Recherche contre la Polyarthrite and the NIH (1R01 AR4146580-01, to D. M. and C. B.), the Arthritis Foundation (I. M.), the Fondation pour la Recherche Médicale and CONICET (M. M.) and the Howard Hughes Medical Institute (D. L.). (AUTHOR – rephrasing OK? Note postdoc fellowship deleted as NI does not allow such citations period.)

## Competing interests statement

The authors declare that they have no competing financial interests.

Received 11 October 2001; accepted 19 February 2002.

1. Lanchbury, J. S. & Pitzalis, C. Cellular immune mechanisms in rheumatoid arthritis and other inflammatory arthritides. *Curr. Biol.* 5, 918–924 (1993).
2. Kouskoff, V. et al. Organ-specific disease provoked by systemic autoreactivity. *Cell* 87, 811–822 (1996).
3. Korganow, A. S. et al. From systemic T cell self-reactivity to organ-specific autoimmune disease via immunoglobulins. *Immunity* 10, 451–461 (1999).

4. Matsumoto, I., Staub, A., Benoist, C. & Mathis, D. Arthritis provoked by linked T and B cell recognition of a glycolytic enzyme. *Science* **286**, 1732–1735 (1999).
5. Basu, D., Horvath, S., Matsumoto, I., Fremont, D. H. & Allen, P. M. Molecular basis for recognition of an arthritic peptide and a foreign epitope on distinct MHC molecules by a single TCR. *J. Immunol.* **164**, 5788–5796 (2000).
6. Maccioni, M. et al. Arthritogenic monoclonal antibodies from K/BxN mice. *J. Exp. Med.* (in the press, 2002). (AUTHOR – do you have details yet?)
7. Ji, H. et al. Arthritis critically dependent on innate immune system players. *Immunity* **16**, 157–168 (2002).
8. West, J. D., Flockhart, J. H., Peters, J. & Bail, S. T. Death of mouse embryos that lack a functional gene for glucose phosphate isomerase. *Genet. Res.* **56**, 223–236 (1990).
9. Frohman, M. A., Dush, M. K. & Martin, G. R. Rapid production of full-length cDNAs from rare transcripts: amplification using a single gene-specific oligonucleotide primer. *Proc. Natl Acad. Sci. USA* **85**, 8998–9002 (1988).
10. Schaller, M., Burton, D. R. & Ditzel, H. J. Autoantibodies to GPI in rheumatoid arthritis: linkage between animal model and human disease. *Nature Immunol.* **2**, 746–753 (2001).
11. Ishikawa, H., Smiley, J. D. & Ziff, M. Electron microscopic demonstration of immunoglobulin deposition in rheumatoid cartilage. *Arthritis Rheum.* **18**, 563–576 (1975).
12. Cooke, T. D., Hurd, E. R., Jasin, H. E., Bienenstock, J. & Ziff, M. Identification of immunoglobulins and complement in rheumatoid articular collagenous tissues. *Arthritis Rheum.* **18**, 541–551 (1975).
13. Vetto, A. A., Mannik, M., Zatarain-Rios, E. & Wener, M. H. Immune deposits in articular cartilage of patients with rheumatoid arthritis have a granular pattern not seen in osteoarthritis. *Rheumatol. Int.* **10**, 13–19 (1990).
14. Pangburn, M. K. in *The Complement System* (eds Rother, K., Till, G. O. & Hansch, G. M.) 93–115 (Springer-Verlag Berlin Heidelberg, 1998).
15. Vivanco, F., Munoz, E., Vidarte, L. & Pastor, C. The covalent interaction of C3 with IgG immune complexes. *Mol. Immunol.* **36**, 843–852 (1999).
16. Shohet, J. M., Pemberton, P. & Carroll, M. C. Identification of a major binding site for complement C3 on the IgG1 heavy chain. *J. Biol. Chem.* **268**, 5866–5871 (1993).
17. Fries, L. F., Gaither, T. A., Hammer, C. H. & Frank, M. M. C3b covalently bound to IgG demonstrates a reduced rate of inactivation by factors H and I. *J. Exp. Med.* **160**, 1640–1655 (1984).
18. Jelezarova, E., Vogt, A. & Lutz, M. U. Interaction of C3b2-IgG complexes with complement proteins properdin, factor B and factor H: implications for amplification. *Biochem. J.* **349**, 217–223 (2000).
19. Schwaeble, W. J. & Reid, K. B. M. Does properdin crosslink the cellular and the humoral immune response? *Immunol. Today* **20**, 17–21 (1999).
20. Fearon, D. T. Regulation by membrane sialic acid of  $\beta$ 1H-dependent decay-dissociation of amplification C3 convertase of the alternative complement pathway. *Proc. Natl Acad. Sci. USA* **75**, 1971–1975 (1978).
21. Meri, S. & Pangburn, M. K. Discrimination between activators and nonactivators of the alternative pathway of complement: regulation via a sialic acid/polyanion binding site on factor H. *Proc. Natl Acad. Sci. USA* **87**, 3982–3986 (1990).
22. Takahashi, S. et al. Cloning and cDNA sequence analysis of nephritogenic monoclonal antibodies derived from an MRL/lpr lupus mouse. *Mol. Immunol.* **30**, 177–182 (1993).
23. Gonzalez, M. L. & Waxman, F. J. Glomerular deposition of immune complexes made with IgG2a monoclonal antibodies. *J. Immunol.* **164**, 1071–1077 (2000).
24. Watanabe, M. et al. Modulation of Renal Disease in MRL/lpr Mice Genetically Deficient in the Alternative Complement Pathway Factor B. *J. Immunol.* **164**, 786–794 (2000).
25. Watanabe, H. et al. Purification of human tumor cell autocrine motility factor and molecular cloning of its receptor. *J. Biol. Chem.* **266**, 13442–13448 (1991).
26. Jeffery, C. J., Bahnson, B. J., Chien, W., Ringe, D. & Petsko, G. A. Crystal structure of rabbit phosphoglucose isomerase, a glycolytic enzyme that moonlights as neuroleukin, autocrine motility factor and differentiation mediator. *Biochemistry* **39**, 955–964 (2000).
27. Sun, Y. J. et al. The crystal structure of a multifunctional protein: phosphoglucose isomerase/autocrine motility factor/neuroleukin. *Proc. Natl Acad. Sci. USA* **96**, 5412–5417 (1999).
28. Wipke, B. T., Wang, Z., Kim, J., McCarthy, T. J. & Allen, P. M. (Title) *Nature Immunol.* **3**, xxx–xxx (2002).
29. Zvaifler, N. J. The immunopathology of joint inflammation in rheumatoid arthritis. *Adv. Immunol.* **265**, 265–336 (1973).
30. Jasin, H. E. Immune mediated cartilage destruction. *Scand. J. Immunol.* **76**, 111–116 (1988).
31. Auffray, C. & Rougeon, F. Purification of mouse immunoglobulin heavy-chain messenger RNAs from total myeloma tumor RNA. *Eur. J. Biochem.* **107**, 303–314 (1980).
32. Ji, H. et al. Genetic influences on the end-stage effector phase of arthritis. *J. Exp. Med.* **194**, 321–330 (2001).

## CASE REPORT

# Significance of magnetic resonance imaging in the diagnosis of nodular regenerative hyperplasia of the liver complicated with systemic lupus erythematosus: a case report and review of the literature

T Horita<sup>1\*</sup>, A Tsutsumi<sup>1,2</sup>, T Takeda<sup>3</sup>, S Yasuda<sup>1</sup>, R Takeuchi<sup>1</sup>, Y Amasaki<sup>1</sup>, K Ichikawa<sup>1</sup>, T Atsumi<sup>1</sup> and T Koike<sup>1</sup>  
<sup>1</sup>Department of Medicine II, Hokkaido University School of Medicine, Sapporo, Japan; <sup>2</sup>Division of Rheumatology, Department of Internal Medicine, Institute of Clinical Medicine, University of Tsukuba, Tsukuba, Japan; and <sup>3</sup>Department of Medicine III, Obihiro Kousei Hospital, Obihiro, Japan

Nodular regenerative hyperplasia of the liver (NRH), characterized by multiple hepatic nodules in the absence of fibrosis, is a rare but important complication of systemic lupus erythematosus (SLE) associated with non-cirrhotic portal hypertension. The diagnosis of NRH is based on the pathological examination, and radiological findings of NRH are poorly documented. We report a case of a 40-year-old woman with SLE complicated with NRH. Sixteen years after diagnosis of SLE, esophageal varices were incidentally found and diagnosis of portal hypertension due to NRH was made by magnetic resonance imaging (MRI) and confirmed by needle liver biopsy. Although MRI showed the lesions as significant nodules, neither computed tomography nor ultrasonography could demonstrate the nodules. However, serial MRI showed significant enlargement of the nodules for 2 years. Because NRH may lead to portal hypertension with life-threatening variceal haemorrhage in patients with SLE, MRI is a useful, non-invasive examination to screen the patients for its presence and follow-up. We reviewed the literature regarding NRH in SLE and discuss the management of the affected patients. *Lupus* (2002) 11, 193–196.

**Key words:** nodular regenerative hyperplasia; portal hypertension; magnetic resonance imaging; systemic lupus erythematosus

## Introduction

Nodular regenerative hyperplasia of the liver (NRH) is defined by diffuse nodular transformation of the hepatic parenchyma without fibrous septa between the nodules,<sup>1</sup> leading to non-cirrhotic portal hypertension, and complicated with systemic lupus erythematosus (SLE) or other autoimmune/haematological diseases, such as Felty's syndrome, rheumatoid arthritis or myeloproliferative diseases.<sup>1–4</sup>

Various hepatic manifestations are common in patients with SLE,<sup>5</sup> but the prevalence of NRH remains unknown. Most patients of NRH are asymptomatic without the elevation of liver enzymes, and the routine radiological examinations, such as com-

puted tomography scan (CT) and ultrasonography (US), hardly show the presence of NRH.

We describe a case of non-cirrhotic portal hypertension complicated with SLE in a 40-year-old female. Her blood transferase levels, CT and US were normal, but magnetic resonance imaging (MRI) demonstrated clear multiple nodules of the liver, diagnosed as NRH. Liver specimens confirmed the presence of regenerated nodules without fibrosis. Since NRH may develop asymptotically and ultimately lead to portal hypertension with fatal variceal haemorrhage, the early diagnosis of NRH is significant to follow-up the affected patients. MRI may be a useful, non-invasive examination to detect NRH in its early stages.

## Case report

A 40-year-old Japanese female was diagnosed as having SLE with manifestations of malar rash, high

\*Correspondence: T Horita, Department of Medicine II, Hokkaido University School of Medicine, N-15, W-7, Kita-ku, Sapporo 060-8638, Japan.

E-mail: thorita@med.hokudai.ac.jp

Received 24 September 2001; accepted 27 November 2001

# B Cells and Immunoglobulins Dependent Mechanisms in Rheumatoid Arthritis: A Possible Rationale of the Extracorporeal Immunomodulation for Rheumatoid Arthritis

Isao Matsumoto and Takayuki Sumida

*Division of Rheumatology, Department of Internal Medicine, Institute of Clinical Medicine, University of Tsukuba, Ibaraki, Japan*

---

**Abstract:** Patients with rheumatoid arthritis (RA) have several options for treatment nowadays, although we do not know what types of therapies are effective for these patients because RA is a very heterogenous disease. We discuss several possible mechanisms of RA in this review and explain one possible scenario of autoantibodies de-

pendent arthritis confirmed by anti-glucose-6-phosphate isomerase antibodies. We also propose several efficacious treatments for treating these patients as *made-to-order* therapies. **Key Words:** Rheumatoid arthritis—B cells—Immunoglobulins—Glucose-6-phosphate isomerase—Made-to-order treatment—Rheumatoid factor.

---

Rheumatoid arthritis (RA) is an important autoimmune disease that inflicts severe pain and disability affecting about 1% of the population in the world. It is also an old disease, putative cases appearing already hundreds of years ago, but RA is still a mysterious disease because there is no consensus on its etiology and pathogenesis. The lack of consensus may depend on these major factors: patients show a range of genetic backgrounds, onset ages, courses of pathology, and responses to therapy. Basically, RA is a chronic, progressive, and symmetrical disease with specific destruction of the synovial joints (1) characterized by leukocyte invasion of the synovial lining and hyperplasia of the resident synoviocytes. The ensuing overproduction of chemokines, cytokines, enzymes, and other soluble mediators provokes neovascularization, cartilage destruction, bone erosion, and anarchic remodeling of joint structures. Systemic manifestations also occur such as increased production of acute phase proteins, vasculitis, and generation of autoantibodies.

To know a scenario of RA pathogenesis, it is nec-

essary to understand what cell types are involved when and what their contributions are. We believe that perhaps RA pathogenesis in these different individuals follows 3 pathways: disease induction, disease perpetuation, and terminal destruction. Of course, not only antigen-dependent mechanisms but also antigen-independent mechanisms might play a key role during all stages of RA because successful treatment with anti-tumor necrosis factor (TNF)-alpha antibodies has recently been proved (2,3). Decades ago, especially in the disease induction and perpetuation state, B cells and immunoglobulins gave way to a T-cell mediated theory, provided by a strong association of particular major histocompatibility complex (MHC) Class II alleles, which was dominant for a number of years. However, the emphasis has shifted again recently to an emphasis on B cells because some arthritogenic immunoglobulins, such as anti-collagen Type II antibodies and anti-glucose-6-phosphate isomerase (GPI) antibodies have been detected from arthritis models of mouse (4,5) and human RA (6,7).

## RHEUMATOID ARTHRITIS MODEL: K/B<sub>x</sub>N MICE

K/B<sub>x</sub>N mice have been described recently as a new model for RA (8). These transgenic mice express a T-cell receptor transgene reactive against the

---

Received March 2002.  
Address correspondence and reprint requests to Dr. Isao Matsumoto, Division of Rheumatology, Department of Internal Medicine, Institute of Clinical Medicine, University of Tsukuba, 1-1-1 Tenodai, Tsukuba City, Ibaraki 305-8575, Japan. E-mail: ismatsu@md.tsukuba.ac.jp

Ag7 MHC-II molecule bound by a self peptide of ubiquitous protein. Surprisingly, transfer of serum or purified serum immunoglobulin (Ig) G antibodies from K/BxN mice into wild-type mice resulted in the onset of arthritis as early as 24 h after transfer (9). Recently, these arthritogenic Igs found in K/BxN serum only recognize a glycolytic enzyme, GPI (5). This anti-GPI antibody induced disease has several similarities with various RA models induced by cartilage proteins, especially collagen induced arthritis because the arthritis is dependent on both T and B cells and transient arthritis can be induced with only anti-collagen II antibodies (4) (mechanisms are summarized in Fig. 1). In fact, there are many similarities: they are dependent on the complement system and inflammatory cytokines (interleukin-1 and TNF-alpha); however, a big discrepancy is found on the localization of the antigen and isotypes of Igs (comparison in Table 1). GPI is a crucial molecule of the glycolytic enzyme, expressed in essentially all tissues from the earliest stages of embryogenesis until death, though with some quantitative variations. It normally resides in cytoplasm, but soluble GPI has been detected in human serum. Of course, a big question still remained: How may antibodies to a ubiquitous cytoplasmic enzyme provoke arthritis? No unusual amounts or sequences, splices, or modification variants of GPI expression were found in joints, although accumulation of extracellular GPI on the lining of the normal cavity, especially along the cartilage surface, was confirmed by immunohistological study (10). This may constitute a generic scenario where, including anti-GPI antibodies, the other antibodies recognizing ubiquitous self-antigens could trigger human arthritis. Indeed, anti-GPI antibodies were increased in 64% of human RA patients but not in controls (7). They also showed that monoclonal anti-GPI IgGs from a patient with RA were highly somatically mutated. These results indicate the immunological events that lead to development of autoimmune disease in the K/BxN mouse model may also occur in human RA. It is possible that regulation of these Igs produced by autoimmune B cells is therapeutically beneficial to human RA.

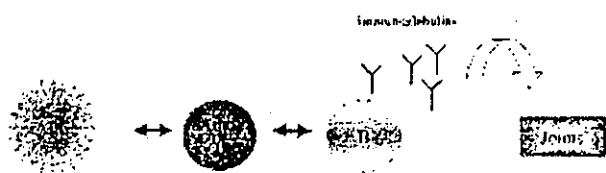


FIG. 1. The drawing shows the mechanisms of autoimmunity in autoantibody dependent arthritis (APC: antigen present cell. Auto T: autoreactive T cells, B: B cells.)

## RHEUMATOID FACTOR IN HUMAN AND ANIMAL MODELS

Rheumatoid factors (RFs) were described initially in 1940 as autoantibodies directed against antigenic determinants on the Fc fragment of IgG. RFs are detected frequently in RA patients (around 70%) and are mainly of IgM, IgG, and IgA isotypes, though also they are found in various other autoimmune diseases and in the healthy population. The frequent occurrence and strong association with RA led to the hypothesis that RFs have arthritogenic functions. Indeed, there were some reports showing that RFs in RA patients were structurally different from other conditions (11), that RF titers correlate with disease activity (12), and that some monoclonal RFs from RA patients bind better to agalactosylated IgGs (13) which was correlated to deficiencies of galactose in serum IgG. However, despite decades of study, the role of RFs in the pathogenesis of RA is still controversial. RFs found in spontaneous and induced animal models may or may not be associated with autoimmune symptoms. In some models, RF production and titers are associated with arthritic symptoms (14) although serum transferred models have not been confirmed.

## TREATMENT OF B CELLS AND IMMUNOGLOBULINS IN RHEUMATOID ARTHRITIS

Recent recommendations for the treatment of RA have focused on early and continued use of disease-modifying antirheumatic drugs and nonsteroidal antiinflammatory drugs. Patients with RA in whom conventional treatments failed have, until recently, had few therapeutic options. These patients would be candidates for more intensive treatments that often are reserved for those with severe disease. Plasmapheresis is one of the options to remove pathogenic components from circulating blood and is used as an adjunct to drug therapy in rheumatoid vasculitis and in some cases of refractory RA. The Pro-sorba column is a medical device that contains highly purified staphylococcal protein A covalently bound to a silica matrix. The Pro-sorba column was approved for the treatment of idiopathic thrombocytopenic purpura and RA in the United States, and the efficacy has been proved by several studies (15). Adsorption of Igs and immune complexes by Pro-sorba might explain this effect although we need to discover the real mechanism of this treatment with further studies. If certain arthritogenic antibodies in humans were confirmed, it is possible that antigen-specific columns might be made for removing these

TABLE 1. Comparison between K/BxN serum and collagen Type II induced arthritis serum

	K/BxN serum	Collagen induced serum
Arthritis onset	24–48 h	24–48 h
Dose of serum	100 $\mu$ l	4 ml
Dose of monoclonal Abs	2 $\times$ 1 mg	3 $\times$ 10 mg
Deposition to tissues	Several organs (synovium, cartilage, spleen, kidney, muscle)	Mainly in joints (cartilage, ears, eyes, trachea, intestine)
Recognition	GPI (277–312) Native form?	Collagen II $\alpha$ -chain (CB-11) Native form?
Pathogenic subtype	IgG1	IgG2a (2b)
Cytokine dependency	IL-1 (TNF- $\alpha$ )	IL-1 (TNF- $\alpha$ )
Complement dependency	C5 alternative pathway	C5

GPI: glucose-6-phosphate isomerase, Ig: immunoglobulin, IL: interleukin, TNF- $\alpha$ : tumor necrosis factor-alpha.

antibodies. Another treatment was done with a monoclonal anti-CD20 antibody; the depletion of B cells seemed to be effective in RA patients (16). These results are consistent with the concept that some categories of patients with RA are critically dependent on B lymphocytes.

### CONCLUSIONS

We summarized the importance of B cells and Igs in RA patients and the possible treatment of B-cell dependent RA. In future studies, we must characterize which patients are B-cell dependent and introduce a clinical test to evaluate B-cell dependency. Also, we need to know something of the genetic relevance to the course of diseases. One of the ways for made-to-order treatment of RA may depend on how we can process them.

### REFERENCES

- Feldmann M, Brennan FM, Maini RN. Rheumatoid arthritis. *Cell* 1996;85:307–10.
- Lipsky PE, van der Heijde DM, St. Clair EW, Furst DE, Breedveld FC, Kalden JR, Smolen JS, Weisman M, Emery P, Feldmann M, Harriman GR, Maini RN; Anti-Tumor Necrosis Factor Trial in Rheumatoid Arthritis with Concomitant Therapy Study Group. Infliximab and methotrexate in treatment of rheumatoid arthritis: Anti-tumor necrosis factor trial in rheumatoid arthritis with concomitant therapy study group. *N Engl J Med* 2000;343:1594–602.
- Bathon JM, Martin RW, Fleischmann RM, Tesser JR, Schiff MH, Keystone EC, Genovese MC, Wasko MC, Moreland LW, Weaver AL, Markenson J, Finck BK. A comparison of etanercept and methotrexate in patients with early rheumatoid arthritis. *N Engl J Med* 2000;343:1586–93.
- Terato K, Hasty KA, Reife RA, Cremer MA, Kang AH, Stuart JM. Induction of arthritis with monoclonal antibodies to collagen. *J Immunol* 1992;148:2103–8.
- Matsumoto I, Staub A, Benoist C, Mathis D. Arthritis provoked by linked T and B cell recognition of a glycolytic enzyme. *Science* 1999;286:1732–5.
- Clauge RB, Moore LJ. IgG and IgM antibody to native type II collagen in rheumatoid arthritis serum and synovial fluid. Evidence for the presence of collagen-anticollagen immune complexes in synovial fluid. *Arthritis Rheum* 1984;27:1370–7.
- Schaller M, Burton DR, Ditzel HJ. Autoantibodies to GPI in rheumatoid arthritis: Linkage between an animal model and human disease. *Nature Immunol* 2001;2:746–53.
- Kouskoff V, Korganow AS, Duchatelle V, Degott C, Benoist C, Mathis D. Organ-specific disease provoked by systemic autoimmunity. *Cell* 1996;87:811–22.
- Korganow AS, Ji H, Mangialaio S, Duchatelle V, Pelanda R, Martin T, Degott C, Kikutani H, Rajewsky K, Pasquali JL, Benoist C, Mathis D. From systemic T cell self-reactivity to organ-specific autoimmune disease via immunoglobulin. *Immunity* 1999;10:451–61.
- Matsumoto I, Maccioni M, Lee DM, Maurice M, Simmons B, Brenner M, Mathis D, Benoist C. How antibodies to a ubiquitous cytoplasmic enzyme may provoke joint-specific autoimmune disease. *Nature Immunol* 2002;3:560–5.
- Thompson KM, Randen I, Borretzen M, Forre O, Natvig JB. Variable region gene usage of human monoclonal rheumatoid factors derived from healthy donors following immunization. *Eur J Immunol* 1994;24:1771–8.
- Shimerling RH, Delbanco TL. The rheumatoid factor: Analysis of clinical utility. *Am J Med* 1991;91:528–34.
- Soltys AJ, Hay FC, Bond A, Axford JS, Jones MG, Randen I, Thompson KM, Natvig JB. The binding of synovial tissue-derived human monoclonal immunoglobulin M rheumatoid factor to immunoglobulin G preparations of differing galactose content. *Scand J Immunol* 1994;40:135–43.
- Hang L, Theofilopoulos AN, Dixon FJ. A spontaneous rheumatoid arthritis-like disease in MRL/l mice. *J Exp Med* 1982;155:1690–701.
- Felson DT, LaValley MP, Baldassare AR, Block JA, Caldwell JR, Cannon GW, Deal C, Evans S, Fleischmann R, Gendreau RM, Harris ER, Matteson EL, Roth SH, Schumacher HR, Weisman MH, Furst DE. The Prosorba column for treatment of refractory rheumatoid arthritis. A randomized, double blind, sham-controlled trial. *Arthritis Rheum* 1999;42:2153–9.
- Edwards JC, Cambridge G. Sustained improvement in rheumatoid arthritis following a protocol design to deplete B lymphocytes. *Rheumatology (Oxford)* 2001;40:205–11.

## Nicked $\beta_2$ -glycoprotein I: a marker of cerebral infarct and a novel role in the negative feedback pathway of extrinsic fibrinolysis

Shinsuke Yasuda, Tatsuya Atsumi, Masahiro Ieko, Eiji Matsuura, Kazuko Kobayashi, Junko Inagaki, Hisao Kato, Hideyuki Tanaka, Minoru Yamakado, Minoru Akino, Hisatoshi Saitou, Yoshiharu Amasaki, Satoshi Jodo, Olga Amengual, and Takao Koike

$\beta_2$ -Glycoprotein I ( $\beta_2$ -GPI) is proteolytically cleaved by plasmin in domain V (nicked  $\beta_2$ -GPI), being unable to bind to phospholipids. This cleavage may occur in vivo and elevated plasma levels of nicked  $\beta_2$ -GPI were detected in patients with massive plasmin generation and fibrinolysis turnover. In this study, we report higher prevalence of elevated ratio of nicked  $\beta_2$ -GPI against total  $\beta_2$ -GPI in patients with ischemic stroke (63%) and healthy subjects with lacunar infarct (27%)

when compared to healthy subjects with normal findings on magnetic resonance imaging (8%), suggesting that nicked  $\beta_2$ -GPI might have a physiologic role beyond that of its parent molecule in patients with thrombosis. Several inhibitors of extrinsic fibrinolysis are known, but a negative feedback regulator has not been yet documented. We demonstrate that nicked  $\beta_2$ -GPI binds to Glu-plasminogen with  $K_D$  of  $0.37 \times 10^{-6}$  M, presumably mediated by the interaction between the fifth domain

of nicked  $\beta_2$ -GPI and the fifth kringle domain of Glu-plasminogen. Nicked  $\beta_2$ -GPI also suppressed plasmin generation up to 70% in the presence of tissue plasminogen activator, plasminogen, and fibrin. Intact  $\beta_2$ -GPI lacks these properties. These data suggest that  $\beta_2$ -GPI/plasmin-nicked  $\beta_2$ -GPI controls extrinsic fibrinolysis via a negative feedback pathway loop. (Blood. 2004; 103:3766-3772)

© 2004 by The American Society of Hematology

### Introduction

$\beta_2$ -Glycoprotein I ( $\beta_2$ -GPI), also known as apolipoprotein H, is a phospholipid-binding plasma protein. Phospholipid-bound  $\beta_2$ -GPI is one of the major target antigens for antiphospholipid antibodies<sup>1-3</sup> present in patients with antiphospholipid syndrome (APS), an autoimmune disorder characterized by arterial/venous thrombosis and pregnancy morbidity.<sup>4</sup>  $\beta_2$ -GPI has 5 homologous short consensus repeats, designated as domains I to V. Domains of  $\beta_2$ -GPI structurally resemble each other, except that domain V has an extra C-terminal loop and a positively charged lysine cluster. In 1993, Hunt et al<sup>5</sup> reported that  $\beta_2$ -GPI is proteolytically cleaved between Lys317 and Thr318 in domain V (nicked  $\beta_2$ -GPI), being unable to bind to phospholipids. This cleavage is generated by factor Xa or by plasmin, with plasmin being more effective.<sup>6</sup>

A large number of reports have detailed the in vitro properties of  $\beta_2$ -GPI as a natural anticoagulant/procoagulant regulator by inhibiting phospholipid-dependent reactions, such as prothrombinase and tenase activity on platelets or phospholipid vesicles,<sup>7,8</sup> factor XII activation,<sup>9</sup> and anticoagulant activity of activated protein C.<sup>10,11</sup> Apart from specific hemostatic functions,  $\beta_2$ -GPI activates lipoprotein lipase,<sup>12</sup> lowers the triglyceride level,<sup>13</sup> binds to oxidized low-density lipoprotein to prevent the progression of atherosclerosis,<sup>14</sup> and binds to nonself particles or apoptotic bodies to allow their clearance.<sup>15-17</sup> Little attention has been given to the functions of the nicked form of  $\beta_2$ -GPI because its phospholipid-

binding activity was thought to exert the physiologic or pathologic functions of  $\beta_2$ -GPI.

Fibrinolytic reactions involve the formation of plasmin from the zymogen plasminogen and the hydrolytic cleavage of fibrin to fibrin degradation products by plasmin. Plasminogen, a 92-kDa glycoprotein, is present in plasma at a concentration of approximately 2  $\mu$ M.<sup>18</sup> Plasminogen consists of 7 domains: one N-terminal peptide, 5 kringle domains bearing a lysine-binding site (LBS) with the capacity to bind fibrin as well as antifibrinolytic proteins carrying lysine, and one serine protease domain.<sup>19</sup> Plasmin conversion from plasminogen by tissue plasminogen activator (tPA) is a key event in extrinsic fibrinolysis for the thrombolysis against intravascular blood clots. Plasmin is one of the most potent enzymes and has a variety of biologic activities; thus, the regulation of plasmin generation and activity is important to maintain the homeostatic balance in vivo. In particular, an excess of fibrinolytic activity can lead to life-threatening bleeding events. Physiologic inhibitors of extrinsic fibrinolysis include  $\alpha_2$ -antiplasmin ( $\alpha_2$ -AP)<sup>20</sup> and plasminogen activator inhibitor 1 (PAI-1).<sup>21</sup> These inhibitors regulate fibrinolysis through different mechanisms.

Nicked  $\beta_2$ -GPI has been identified by sandwich enzyme-linked immunosorbent assay (ELISA) in plasma of patients with disseminated intravascular coagulation (DIC)<sup>22</sup> or leukemia,<sup>23</sup> both conditions characterized by massive thrombin generation and fibrinolytic

From the Department of Medicine II, Hokkaido University Graduate School of Medicine, Sapporo, Japan; Department of Internal Medicine, School of Dentistry, Health Sciences University of Hokkaido, Ishikari-Tobetsu, Hokkaido, Japan; Department of Cell Chemistry, Institute of Molecular and Cellular Biology, Okayama University Medical School, Okayama, Japan; National Cardiovascular Center Research Institute, Osaka, Japan; Narita R&D Center, Iatron laboratories Inc, Mito, Chiba, Japan; Department of Medicine, Mitsui Memorial Hospital, Tokyo, Japan; Department of Neurosurgery, Azabu Neurosurgical Hospital, Sapporo, Japan.

Submitted August 7, 2003; accepted January 5, 2004. Prepublished online as *Blood* First Edition Paper, January 15, 2004; DOI 10.1182/blood-2003-08-2712.

Supported in part by grants from the Japanese Ministry of Health, Labour and Welfare, by those from the Japanese Ministry of Education, Culture, Sports, Science and Technology, and by the Sankyo Foundation of Life Science.

Reprints: Tatsuya Atsumi, Department of Medicine II, Hokkaido University Graduate School of Medicine, N15, W7, Kita-ku, Sapporo 060-8638, Japan; e-mail: at31at@med.hokudai.ac.jp.

The publication costs of this article were defrayed in part by page charge payment. Therefore, and solely to indicate this fact, this article is hereby marked "advertisement" in accordance with 18 U.S.C. section 1734.

© 2004 by The American Society of Hematology

turnover. To investigate the biologic and clinical significance of nicked  $\beta_2$ -GPI in a disease characterized by a lower level of thrombin generation and fibrin turnover than DIC, we evaluated the cleavage ratio of  $\beta_2$ -GPI in plasma of patients with ischemic stroke and the results are presented herein. Further, we investigated the role of nicked  $\beta_2$ -GPI in extrinsic fibrinolysis and demonstrate for the first time that nicked  $\beta_2$ -GPI binds to plasminogen. We also describe the inhibitory effect of nicked  $\beta_2$ -GPI on the fibrin surface where plasminogen is proteolytically activated into plasmin. Because  $\beta_2$ -GPI may be cleaved *in vivo* by plasmin during thrombus formation and thrombolysis, these phenomena represent a novel negative feedback loop in extrinsic fibrinolysis where  $\beta_2$ -GPI plays a key role.

## Patients, materials, and methods

### Study patients

The study population comprised 62 patients with history of ischemic stroke diagnosed by magnetic resonance imaging (MRI) performed at the time of admission to the Azabu Neurosurgical Hospital (female-to-male ratio, 12:50; mean age,  $68 \pm 9$  years). Blood samples were obtained from the patients at least 6 months after their last occlusive event.

We also investigated 130 age- and sex-matched apparently healthy subjects with no history of cerebral infarct who consented to join the study. All subjects underwent a cerebral MRI at the Neuroradiology Department at Mitsui Memorial Hospital and images were analyzed by an experienced neuroradiologist. According to the MRI findings the healthy subjects were divided into 2 groups: 52 with lacunar infarcts (female-to-male ratio, 20:32; mean age  $67 \pm 9$  years) and 78 without any abnormality (female-to-male ratio, 26:52; mean age,  $66 \pm 6$  years). Blood sampling was performed at the same time of the MRI scan. All the patients and healthy volunteers provided informed consent according to Declaration of Helsinki principles.

### Blood collection

Venous blood was collected in tubes containing one-tenth volume of 0.105 M sodium citrate and was centrifuged immediately at  $4^\circ\text{C}$ . Plasma samples were depleted of platelets by filtration then stored at  $-70^\circ\text{C}$  until use.

### Materials

**Monoclonal antibodies.** To measure the plasma levels of nicked or total  $\beta_2$ -GPI, we used 2 monoclonal antibodies, 1 monoclonal anti-nicked  $\beta_2$ -GPI antibody (NGPI-60) that specifically reacts against nicked  $\beta_2$ -GPI and the other monoclonal anti- $\beta_2$ -GPI antibody (NGPI-23) that equally reacts with nicked and intact  $\beta_2$ -GPI.<sup>23</sup>

An IgG mouse monoclonal antihuman  $\beta_2$ -GPI antibody directed to domain III of human  $\beta_2$ -GPI (Cof-22) was used for the purification of nicked  $\beta_2$ -GPI and evaluation of the binding of nicked  $\beta_2$ -GPI to immobilized Glu-plasminogen.<sup>24</sup> Cleavage of  $\beta_2$ -GPI by plasmin did not affect the binding of Cof-22 to  $\beta_2$ -GPI because the epitope of Cof-22 antibody on  $\beta_2$ -GPI molecule resides on domain III (data not shown).

Antihuman plasminogen antibodies directed to kringles 1 to 3 or against kringle 4 were obtained from American Diagnostica (Greenwich, CT).

**Proteins.**  $\beta_2$ -GPI was purified from human plasma, as described.<sup>25</sup> Nicked  $\beta_2$ -GPI was prepared as reported<sup>26</sup> with slight modifications that included an additional purification step:  $\beta_2$ -GPI was treated with human plasmin (Calbiochem-Novabiochem, La Jolla, CA) at  $37^\circ\text{C}$  for 3 hours, at a molar ratio of  $\beta_2$ -GPI/plasmin of 5:1. Plasmin-treated  $\beta_2$ -GPI was first purified on a Cof 22-Sepharose column and subsequently on a heparin-Sepharose column. The heparin nonbinding fraction was collected and further purified by ion-exchange chromatography using Mono-Q column (Pharmacia Biotech, Uppsala, Sweden). Purified  $\beta_2$ -GPI was reduced using 2-mercaptoethanol and subjected to sodium dodecyl sulfate-polyacrylamide gel electrophoresis (SDS-PAGE), appearing as a single band smaller than that of the intact one (data not shown).

The domain V-deleted mutant protein (domains I-IV) of  $\beta_2$ -GPI was expressed using a baculovirus system as reported.<sup>24</sup> This mutant  $\beta_2$ -GPI does not include the cleavage site for plasmin.

Glu-plasminogen was purified from the plasma of healthy Japanese donors using chromatography on lysine-Sepharose 4B (Pharmacia Biotech) and diethylaminoethyl (DEAE) Sephadex A-50 (Pharmacia Biotech). Plasminogen kringles 1 to 3 fragment, plasminogen kringle 4 fragment, and mini-plasminogen, which consists of the kringle 5 and serine protease domain of plasminogen, were obtained from Technoclone (Vienna, Austria). Recombinant tPA (2-chain, Duteplase) was obtained from Sumitomo Pharmaceutical (Osaka, Japan).  $\epsilon$ -Aminocaproic acid (EACA) was purchased from Sigma Chemical (St Louis, MO).

### Methods

**Measurement of plasma levels of nicked  $\beta_2$ -GPI.** Plasma levels of nicked  $\beta_2$ -GPI were determined by a sandwich ELISA as previously described with slight modifications.<sup>25</sup> Briefly, polystyrene microtiter plates were coated with 100  $\mu\text{L}$  monoclonal anti-nicked  $\beta_2$ -GPI antibody (NGPI-60) in 50 mM Tris (tris(hydroxymethyl)aminomethane)-HCl, pH 7.5, containing 0.15 M NaCl and incubated overnight at  $4^\circ\text{C}$ . Wells were washed 3 times with 0.5 M NaCl containing 0.05% Tween 20 and 100  $\mu\text{L}$  citrated plasma samples diluted 5-fold in 20 mM Tris-HCl, pH 7.5, containing 0.5 M NaCl and 0.05% Tween 20 (sample buffer) were added. After 2 hours of incubation at room temperature and washing 3 times, 100  $\mu\text{L}$  biotinylated F(ab')<sub>2</sub> fragment of monoclonal anti- $\beta_2$ -GPI (NGPI-23; 2  $\mu\text{g}/\text{mL}$ ) was added to each well, followed by 1 hour of incubation. Then, 100  $\mu\text{L}$  alkaline phosphatase (ALP)-conjugated streptavidin (Zymed, San Francisco, CA) at a 1:1000 dilution in sample buffer was added to each well. After another 1 hour of incubation and 3 times washing, 200  $\mu\text{L}$  substrate (1 mg/mL p-nitrophenylphosphate disodium [Sigma Chemical] in 1 M diethanolamine buffer [pH 9.8]) was added. Optical density (OD) was read at 492 nm with reference at 620 nm using an ELISA plate reader. The plasma levels of nicked  $\beta_2$ -GPI were determined from a standard curve constructed with citrated plasma spiked with known amounts of purified nicked  $\beta_2$ -GPI.

**Measurement of plasma levels of total  $\beta_2$ -GPI.** Plasma levels of total  $\beta_2$ -GPI were determined by a sandwich ELISA using F(ab') fragment of NGPI-23 as the capture antibody and biotinylated antihuman  $\beta_2$ -GPI rabbit IgG as the tag antibody as previously reported.<sup>25</sup> Plasma samples of 50  $\mu\text{L}$  (5000-fold diluted) were added to the wells containing the immobilized antibody. The ALP-conjugated streptavidin (Zymed) was then added and bound ALP was determined as described ("Measurement of plasma levels of nicked  $\beta_2$ -GPI"). The amounts of total  $\beta_2$ -GPI in plasma were calculated from a calibration curve constructed with known amounts of purified  $\beta_2$ -GPI. A nicked  $\beta_2$ -GPI ratio was calculated in all samples using the formula: (plasma nicked  $\beta_2$ -GPI/plasma total  $\beta_2$ -GPI)  $\times$  1000.

**Other laboratory investigations.** The same plasma samples were tested for thrombin-antithrombin (TAT) complexes, plasmin-antiplasmin (plasmin inhibitor) complex (PPI), and D-dimers (DDs) by latex agglutination assay using commercial kits LPIAACE TAT, LPIAACE PPI, LPIAACE D-D dimer (Dia-Iatron, Tokyo, Japan), according to the manufacturer's instructions.

**ELISA for binding of intact or nicked  $\beta_2$ -GPI to plasminogen.** The binding of nicked or intact  $\beta_2$ -GPI was investigated by ELISA. Fifty microliters of Glu-plasminogen (10  $\mu\text{g}/\text{mL}$ ) in phosphate-buffered saline (PBS), pH 7.4, was distributed in each well of a Sumilon Type S microtiter ELISA plate (Sumitomo Bakelite, Tokyo, Japan) and incubated overnight at  $4^\circ\text{C}$ . After washing twice with PBS and blocking with 2% gelatin-PBS for 1 hour at  $37^\circ\text{C}$ , 50  $\mu\text{L}$  of serial dilutions of intact or nicked  $\beta_2$ -GPI in 1% bovine serum albumin (Sigma Chemical)-PBS (1% BSA-PBS) were placed in each well. Plates were incubated for 1 hour at room temperature and washed 3 times with PBS containing 0.05% Tween 20 (PBS-Tween), then 50  $\mu\text{L}/\text{well}$  Cof-22 (100 ng/mL) in 1% BSA-PBS was distributed. After incubation and washing as above, 50  $\mu\text{L}/\text{well}$  of ALP-conjugated anti-mouse IgG (Sigma Chemical), diluted 1:2000 in 1% BSA-PBS, was put into each well, followed by incubation. Substrate (100  $\mu\text{L}$ ) was distributed after washing 4 times with PBS-Tween and incubated. OD was read at 405 nm with reference at 620 nm.



The role of plasminogen LBS in binding to nicked  $\beta_2$ -GPI was evaluated by a competitive ELISA adding serial dilutions of EACA, a lysine analog, into the nicked  $\beta_2$ -GPI solution.

**Kinetic assay for molecular interaction between nicked  $\beta_2$ -GPI and plasminogen.** Real-time analysis for molecular interaction between nicked  $\beta_2$ -GPI and Glu-plasminogen was performed using an optical-biosensor, IA-sys system (Affinity Sensors, Paramus, NJ). Biotinylated Glu-plasminogen was immobilized on the wall of a biotin cuvette (Affinity Sensors) via streptavidin (Sigma Chemical). After blocking with 0.01% BSA-PBS and washing with PBS, various concentrations (up to 4  $\mu$ M) of native or nicked  $\beta_2$ -GPI were placed in the cuvette and ligand bound to the plasminogen-coated surface was detected. Obtained data were fitted using linear regression to find the intercept and gradient. This analysis was used to determine the association rate constant ( $k_{\text{ass}}$ ) and dissociation rate constant ( $k_{\text{diss}}$ ), from the variation of the on-rate constant ( $k_{\text{on}}$ ) with ligand concentration. According to the equation:  $k_{\text{on}} = k_{\text{diss}} + k_{\text{ass}}[\text{ligand}]$ ,  $K_D$  and  $K_A$  are determined as follows:  $K_D = k_{\text{diss}}/k_{\text{ass}}$  and  $K_A = k_{\text{ass}}/k_{\text{diss}}$ .

**Inhibition ELISA.** To identify the nicked  $\beta_2$ -GPI-binding site on Glu-plasminogen, the inhibition of Glu-plasminogen binding by fragments of plasminogen was examined. Fifty microliters of nicked  $\beta_2$ -GPI (0.2  $\mu$ M) diluted in PBS was put into each well of a MaxiSorp microtiter plate (Nalge Nunc International, Roskilde, Denmark) and incubated overnight at 4°C. After washing twice with PBS and blocking with 2% gelatin-PBS for 1 hour at 37°C, serial dilutions of inhibitor (BSA, plasminogen kringle 1-3, plasminogen kringle 4, or mini-plasminogen) were added (50  $\mu$ L/well) followed by overnight incubation at 4°C. After washing with PBS-Tween, 10  $\mu$ g/mL Glu-plasminogen was then added (50  $\mu$ L/well) and incubated for 30 minutes at room temperature, and plates were washed 3 times with PBS-Tween. To compare the inhibitory effect between kringle 1 to 3 and mini-plasminogen, a monoclonal anti-kringle 4 antibody (American Diagnostica) was used to detect bound Glu-plasminogen, whereas a monoclonal anti-kringle 1 to 3 antibody (American Diagnostica) was used to compare the inhibition of mini-plasminogen with that of kringle 4. After incubation with these monoclonal antibodies, bound Glu-plasminogen on nicked  $\beta_2$ -GPI was evaluated by ALP-conjugated antimouse IgG, followed by substrate addition as described ("ELISA for binding of intact or nicked  $\beta_2$ -GPI to plasminogen").

**Inhibitory effect of nicked  $\beta_2$ -GPI on the binding of plasminogen to fibrin.** To investigate whether nicked  $\beta_2$ -GPI interferes with the binding of Glu-plasminogen to immobilized fibrin in a liquid phase or not, the following experiment was done. Each well of a Sumilon Type S microtiter plate (Sumitomo Bakelite) was coated with soluble fibrin monomer (5  $\mu$ g/mL) and incubated at 4°C overnight, followed by washing with PBS-Tween and blocking with 2% gelatin-PBS at 37°C. Biotinylated Glu-plasminogen (5  $\mu$ g/mL in 1% BSA-PBS) was preincubated with different concentrations of intact or nicked  $\beta_2$ -GPI for 1 hour at room temperature and added to the wells in triplicate. After incubation for 1 hour at room temperature, each well was washed with PBS-Tween. ALP-conjugated streptavidin was diluted to 3000 times in PBS and distributed to the wells. After 1 hour of incubation and washing, substrate was added and absorbance was measured as described.

**Effects of intact or nicked  $\beta_2$ -GPI on tPA activity: chromogenic assay.** In the presence of fibrin, tPA can effectively activate plasminogen to plasmin. Because we speculated that nicked  $\beta_2$ -GPI might interfere with this activation step by binding to plasminogen, chromogenic assay measuring plasmin generation was introduced in the presence of tPA, Glu-plasminogen, fibrin monomer, and  $\beta_2$ -GPI. The effect of intact/nicked  $\beta_2$ -GPI on the activity of plasmin generated was evaluated using a parabolic rate assay. The activity of tPA was measured in a chromogenic assay as described<sup>27</sup> with some modifications. A mixture of the same volume of 50 U/mL tPA in PBS and 1 M acetate buffer (pH 3.9) was incubated for 5 minutes at room temperature, then diluted 1:160 with assay buffer (50 mM Tris-HCl, pH 8.8, 100 mM NaCl, and 0.01% Triton X-100). Then 100  $\mu$ L of the diluted tPA solution was incubated in a Sumilon Type S microtiter plate with 100  $\mu$ L detection reagents consisting of Glu-plasminogen and plasmin-sensitive substrate (Glu-plasminogen [70  $\mu$ g/mL] and 0.6 mM chromogenic substrate S-2251 [Chromogenix, Möndal, Sweden] in assay buffer) with intact or nicked  $\beta_2$ -GPI and 2  $\mu$ L/well soluble fibrin monomer

(3.3 mg/mL in 3.5 M urea). The final concentrations of intact/nicked  $\beta_2$ -GPI were 0, 0.25, and 0.5  $\mu$ M. Domain I to IV of  $\beta_2$ -GPI mutant or BSA served as the negative control. After incubation at 37°C for 12 hours, the activity of plasmin generated was determined by measuring absorbance at 405 nm using a microplate reader (model 3550; BioRad, Hercules, CA). A standard curve was generated using serial dilutions of tPA. The plasmin generation in this system was expressed as corresponding tPA activity (U/mL).

**Effects of intact or nicked  $\beta_2$ -GPI on tPA activity: fibrin plate assay.** To exclude the possibility that nicked  $\beta_2$ -GPI affected S-2251 cleavage without interacting with fibrinolytic factors, fibrinolysis was evaluated by conventional fibrin plate assays. Fibrin was layered on a plastic plate 10 cm in diameter, using the same volumes of 0.2% plasminogen-free fibrin (Sigma Chemical), 1% agarose, and 200  $\mu$ L/plate thrombin, 20 U/mL. Then, 6  $\mu$ L of the diluted tPA solution ("Effects of intact or nicked  $\beta_2$ -GPI on tPA activity: chromogenic assay") was incubated with the same volume of Glu-plasminogen (70  $\mu$ g/mL) in assay buffer, with intact or nicked  $\beta_2$ -GPI (up to 0.5  $\mu$ M). After 36 hours of incubation at 37°C, the area of lysis rings was measured. A standard curve was generated from serial dilutions of tPA.

**Statistical analysis.** Statistical evaluation was performed by the *t* test, Fisher exact test,  $\chi^2$  test, or Spearman rank correlation as appropriate. *P* values less than .05 were considered statistically significant.

## Results

### Levels of nicked $\beta_2$ -GPI in plasma samples

The plasma levels of nicked  $\beta_2$ -GPI ratio are shown in Figure 1. A normal level of nicked  $\beta_2$ -GPI ratio was derived from the apparently healthy subjects without any MRI abnormality, the mean plus 1 SD representing the upper limit of normal. A higher prevalence of elevated nicked  $\beta_2$ -GPI ratio was found in patients with ischemic stroke (63%, 39 of 62) and healthy subjects with lacunar infarct (27%, 14 of 52) when compared to healthy subjects with normal MRI findings (8%, 6 of 78). Relative risks of having stroke or asymptomatic lacunar infarction were approximated by odds ratio (95% CI), 20.3 (7.6-54.2) and 4.4 (1.6-12.4), respectively.

The prevalence of elevated levels of markers of thrombin generation and fibrinolytic turnover in our population are shown in Figure 2. A statistically significant correlation was observed between levels of PPI and nicked  $\beta_2$ -GPI ratio in plasma of healthy subjects with lacunar infarct ( $r^2 = 0.31$ ,  $P = .02$ ). No correlations were found between nicked  $\beta_2$ -GPI ratio and DDs or TAT complexes in any of the groups.

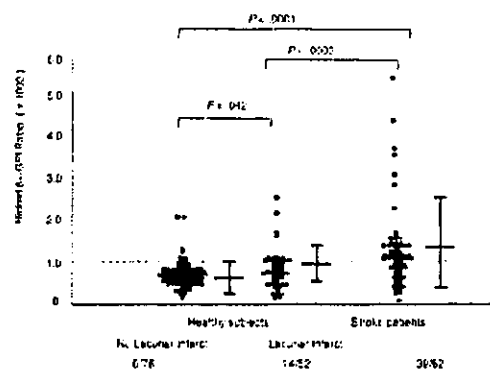


Figure 1. Plasma levels of nicked  $\beta_2$ -GPI. Total and nicked  $\beta_2$ -GPI plasma levels were determined by ELISA. A nicked  $\beta_2$ -GPI ratio, (plasma nicked  $\beta_2$ -GPI/plasma total  $\beta_2$ -GPI)  $\times$  1000, was established in all the samples. The dashed line indicates the mean + 1 SD of the ratio in healthy subjects without lacunar infarct. *P* values were calculated using *t* test.

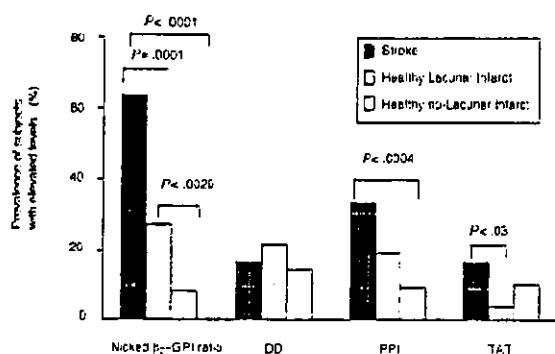


Figure 2. Prevalence of abnormally elevated plasma levels of nicked  $\beta_2$ -GPI and of markers of thrombin generation/fibrinolytic turnover in our population. Plasma levels of D-dimers (DD), plasmin-antiplasmin complex (PPI), and thrombin-antithrombin complexes (TAT) were determined in all the subjects as described in "Patients, materials, and methods."

In the apparently healthy subjects group ( $n = 130$ ), plasma nicked  $\beta_2$ -GPI ratio significantly correlated with age ( $r^2 = 0.483$ ,  $P < .0001$ ; Figure 3). Therefore, plasma measurement of nicked  $\beta_2$ -GPI might be a useful screening tool in the assessment of patients at risk of ischemic stroke.

#### Binding of nicked $\beta_2$ -GPI to Glu-plasminogen

The binding of up to  $0.4 \mu\text{M}$  nicked  $\beta_2$ -GPI to solid-phase Glu-plasminogen occurred in a dose-dependent manner, whereas the same concentrations of intact  $\beta_2$ -GPI did not bind to Glu-plasminogen (Figure 4A). The binding of Cof-22 to  $\beta_2$ -GPI was not affected by the cleavage of  $\beta_2$ -GPI. Molecular interaction between intact or nicked  $\beta_2$ -GPI and plasminogen was investigated using an optical biosensor. Nicked  $\beta_2$ -GPI showed a large extent of binding to immobilized Glu-plasminogen, whereas intact  $\beta_2$ -GPI did not show any specific binding (Figure 4B). The data of  $k_{on}$  at different concentrations of nicked  $\beta_2$ -GPI were fitted using linear regression, determining  $k_{on}$  as  $0.0006 \text{ M}^{-1}\text{s}^{-1}$  and  $k_{off}$  as  $0.0022 \text{ s}^{-1}$  (Figure 4C). Accordingly,  $K_D$  and  $K_A$  were determined as  $0.37 \times 10^{-6} \text{ M}$  and  $2.70 \times 10^6 \text{ M}^{-1}$ , respectively.

#### Inhibition of binding of Glu-plasminogen to nicked $\beta_2$ -GPI by the fragments of plasminogen or by EACA

The binding of Glu-plasminogen ( $10 \mu\text{g/mL}$ ) to immobilized nicked  $\beta_2$ -GPI, but not to native  $\beta_2$ -GPI, was demonstrated by ELISA. For the inhibition assay, the fragments of plasminogen (mini-plasminogen or kringle 4) as the inhibiting factors were added to the wells coated with nicked  $\beta_2$ -GPI, and bound Glu-plasminogen was detected using a monoclonal antikringle 1 to 3 antibody. Mini-plasminogen, but not kringle 4, inhibited the binding between Glu-plasminogen and nicked  $\beta_2$ -GPI (Figure 5A). Kringle 1 to 3 fragment or mini-plasminogen was added as inhibitor and bound Glu-plasminogen was detected using a monoclonal antikringle 4 antibody. Glu-plasminogen binding to nicked  $\beta_2$ -GPI was dose dependently inhibited by mini-plasminogen but not by kringle 1 to 3 fragment (Figure 5B). The fifth domain or the catalytic domain of Glu-plasminogen, therefore, was predicted to mediate its binding to nicked  $\beta_2$ -GPI.

When the binding of nicked  $\beta_2$ -GPI ( $10 \mu\text{g/mL}$ ) to solid-phase Glu-plasminogen was tested in the presence of different concentrations of EACA, the binding between nicked  $\beta_2$ -GPI and immobilized Glu-plasminogen was abolished in a dose-dependent manner (Figure 5C). Accordingly, LBS on plasminogen might mediate the binding of nicked  $\beta_2$ -GPI to Glu-plasminogen.

#### Binding of plasminogen to fibrin interfered with by nicked $\beta_2$ -GPI

We also investigated whether nicked  $\beta_2$ -GPI has an effect on the binding of Glu-plasminogen to immobilized fibrin monomer using an ELISA system. After preincubation with nicked  $\beta_2$ -GPI, but not with intact  $\beta_2$ -GPI, Glu-plasminogen showed decreased binding activity to soluble fibrin monomer (Figure 5D).

#### Effects of nicked $\beta_2$ -GPI on extrinsic fibrinolysis

The amidolytic activity of newly generated plasmin was evaluated as tPA activity (U/mL) in a chromogenic assay. The activity increased with the concentration of tPA (data not shown). When nicked  $\beta_2$ -GPI was added, the tPA activity decreased in a dose-dependent manner (Figure 6A). Intact  $\beta_2$ -GPI at  $0.25 \mu\text{M}$  did not suppress the fibrinolytic activity, whereas intact  $\beta_2$ -GPI in a higher concentration ( $0.50 \mu\text{M}$ ) slightly suppressed the fibrinolytic activity. The same amount of BSA or the recombinant domain I to IV of  $\beta_2$ -GPI did not affect the tPA activity.

The fibrinolytic activity of generated plasmin was measured as tPA activity (U/mL) in a fibrin plate assay. Fibrinolytic activity was suppressed by nicked  $\beta_2$ -GPI at  $0.25$  and  $0.50 \mu\text{M}$ . Intact  $\beta_2$ -GPI at  $0.50 \mu\text{M}$  also slightly inhibited the fibrinolytic activity. However,  $0.25 \mu\text{M}$  intact  $\beta_2$ -GPI did not affect the fibrinolytic activity of tPA (Figure 6B).

## Discussion

In the first part of this study, we demonstrated that plasma levels of nicked  $\beta_2$ -GPI were elevated in patients with ischemic stroke, indicating an elevated degree of fibrin turnover, but lower than that of DIC where thrombin and plasmin are massively generated.

In fact, nicked  $\beta_2$ -GPI was detected in large quantities in plasma of patients with DIC, a pathologic state characterized by marked increase of plasma PPI.<sup>22</sup> We observed a strong correlation between plasma levels of nicked  $\beta_2$ -GPI and those of PPI in the healthy individuals showing lacunar infarcts on MRI, suggesting that nicked  $\beta_2$ -GPI may rather reflect "minor" plasmin generation. In the presence of larger plasmin generation, the correlation between nicked  $\beta_2$ -GPI and PPI may be lost,<sup>23</sup> presumably due to the consumption of  $\alpha_2$ -AP. In individuals with MRI abnormalities the prevalence of increased nicked  $\beta_2$ -GPI ratio was higher than that of PPI, DDs, and TAT complexes (46%, 27%, 19%, and 11%, respectively). Thus, the detection of nicked  $\beta_2$ -GPI may

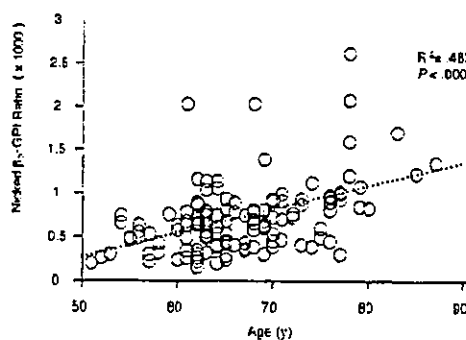
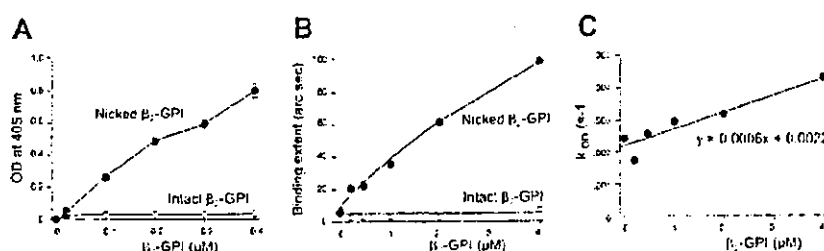


Figure 3. Correlation between plasma levels of nicked  $\beta_2$ -GPI and age in apparently healthy subjects. Nicked  $\beta_2$ -GPI was measured by a sandwich ELISA. The dotted line represents the regression curve. Each circle shows nicked  $\beta_2$ -GPI ratio and age in each subject.



**Figure 4.** Binding of intact/nicked  $\beta_2$ -GPI to Glu-plasminogen. (A) Binding of intact or nicked  $\beta_2$ -GPI to immobilized Glu-plasminogen was evaluated by ELISA using mouse monoclonal anti- $\beta_2$ -GPI antibody Cof-22. Closed circles indicate the dose-dependent binding of nicked  $\beta_2$ -GPI to Glu-plasminogen, whereas open circles indicate that intact  $\beta_2$ -GPI is unable to bind to Glu-plasminogen. (B-C) Kinetic plot showing molecular interaction between Glu-plasminogen and intact or nicked  $\beta_2$ -GPI. Intact  $\beta_2$ -GPI or nicked  $\beta_2$ -GPI binding to Glu-plasminogen was detected using IAsys, an optical biosensor as described in "Patients, materials, and methods." Binding extent (arc sec) was compared between intact and nicked  $\beta_2$ -GPI (B). Obtained on-rate constant ( $k_{on}$ ) for nicked  $\beta_2$ -GPI was plotted and fitted using linear regression to find the intercept and gradient (C). A formula for determining the association rate constant ( $k_{ass}$ ) and dissociation rate constant ( $k_{diss}$ ) is as follows:  $k_{on} = k_{ass} + k_{diss} [\text{ligand}]$ . Error bars indicate SDs.

represent a more sensitive marker of vascular lesions than PPI, DDs, or TAT complexes.

In support of this concept is the correlation between nicked  $\beta_2$ -GPI ratio and age in the apparently healthy subjects, suggesting that "minor" plasmin generation might be associated with subclinical or early clinical atherosclerosis. It is widely accepted that atherosclerosis is associated with endothelial cell activation and minor plaque rupture leading to small thrombus formation, secretion of t-PA, and plasmin generation, ultimately cleaving  $\beta_2$ -GPI. Indeed, nicked  $\beta_2$ -GPI can be generated on the surface of activated endothelial cells or platelets.<sup>23</sup>

In the second part of this study, we investigated the properties of nicked  $\beta_2$ -GPI *in vivo* to evaluate the biologic significance of our observations. We showed that nicked  $\beta_2$ -GPI specifically binds to Glu-plasminogen and inhibits extrinsic fibrinolysis *in vitro*. In contrast, neither domain I to IV of  $\beta_2$ -GPI nor intact  $\beta_2$ -GPI revealed such functions. The administration of intact  $\beta_2$ -GPI in higher concentrations also suppressed plasmin generation, perhaps owing to the nicked  $\beta_2$ -GPI produced by the newly generated plasmin. Under clinical conditions characterized by massive plasmin generation such as DIC or acute thrombosis, plasmin is generated by tPA released from activated endothelial cells with thrombus formation, and plasmin cleaves  $\beta_2$ -GPI on the thrombus, changing the properties of  $\beta_2$ -GPI. We propose that  $\beta_2$ -GPI is a precursor of plasmin-nicked  $\beta_2$ -GPI, a physiologic inhibitor of fibrinolysis.

The crystal structure of human  $\beta_2$ -GPI has been defined.<sup>26,29</sup> Bouma et al<sup>26</sup> proposed that a large positively charged patch in domain V binds to anionic surfaces with a flexible and partially

hydrophobic loop inserted into the lipid layer. According to the conformation of the nicked domain V, as predicted from the x-ray structure of the intact domain V and confirmed by heteronuclear magnetic resonance, the nicked C-terminal loop is tightly fixed by electrostatic interaction with enhanced stability, the result being neutralization of the positive charge of the lysine cluster.<sup>26,30</sup>

Glu-plasminogen, a full-length protein, is the naturally circulating form of plasminogen. Kringle 5 of Glu-plasminogen has a higher affinity for intact fibrin.<sup>31,32</sup> LBS in kringle 5 of Glu-plasminogen mediates its binding to N-terminal lysine on fibrin, an event essential to initiate fibrinolysis reactions. This initial binding of Glu-plasminogen to fibrin induces a conformational change from a "closed" to an "open" form, thus promoting accessibility to plasminogen activators such as tPA or urokinase.<sup>19</sup> On the fibrin surface, generated plasmin cleaves the single-chain tPA into the 2-chain tPA, a more active form, providing a positive feedback for plasmin generation. Plasmin simultaneously degrades fibrin and makes C-terminal lysine of fibrin more accessible to plasminogen via kringles 1,<sup>33,34</sup> 2, and 3,<sup>35</sup> thus accelerating fibrinolysis.

According to the results of the inhibition studies using plasminogen fragments or EACA (Figure 5), and comparison of the effect on plasmin generation between nicked  $\beta_2$ -GPI and domain I to IV of  $\beta_2$ -GPI (Figure 6A), it would be indicated that the binding of nicked  $\beta_2$ -GPI to Glu-plasminogen is mediated by the interaction between the lysine-cluster patch in domain V of the nicked  $\beta_2$ -GPI and LBS on the plasminogen kringle 5,<sup>36</sup> although it still may be possible that an excess amount of EACA interacts with the catalytic domain of Glu-plasminogen. The conformational difference between intact and nicked  $\beta_2$ -GPI is critical for its binding to

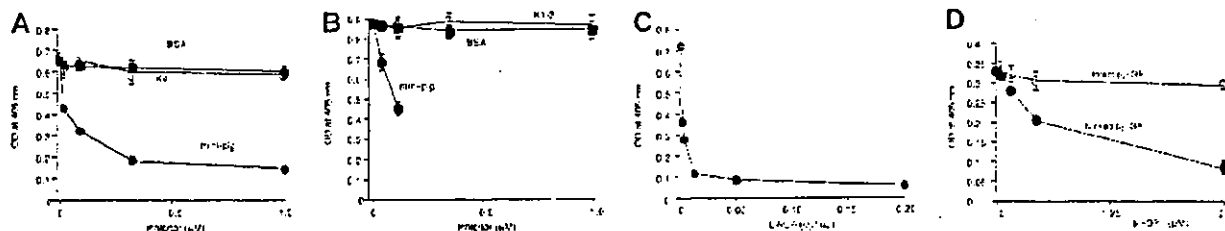


**Figure 5.** Identification of the binding site of Glu-plasminogen to  $\beta_2$ -GPI by inhibition ELISA using plasminogen fragments. (A) Binding of Glu-plasminogen to immobilized nicked  $\beta_2$ -GPI was tested by ELISA in the presence of possible inhibitors. After nicked  $\beta_2$ -GPI immobilization onto microtiter plates, different concentrations of kringle 4 of plasminogen (C) or mini-plasminogen (that consists of kringle 5 and catalytic domain of plasminogen; ●) were added as inhibitors. BSA (■) served as control. After incubation and washing, Glu-plasminogen (10  $\mu\text{g/mL}$ ) was added and bound Glu-plasminogen was determined using kringle 1- to 3-specific mouse monoclonal antiplasminogen antibody. (B) For the inhibition ELISA kringle 1 to 3 of plasminogen (C) or mini-plasminogen (●) served as inhibitors. Glu-plasminogen bound to immobilized  $\beta_2$ -GPI was detected using kringle 4-specific mouse monoclonal antiplasminogen antibody. Assays were run in triplicate. (C) Competitive ELISA using EACA, a lysine homologue. Binding of nicked  $\beta_2$ -GPI (0.2  $\mu\text{M}$ ) to immobilized Glu-plasminogen was tested by ELISA using Cof-22 antibody in the presence of various concentrations of EACA (0-0.20  $\mu\text{g/mL}$ ). (D) Soluble fibrin monomer (5  $\mu\text{g/mL}$ ) was coated on the surface of a microtiter plate and blocked. Biotinylated Glu-plasminogen (5  $\mu\text{g/mL}$ ) was preincubated with intact or nicked  $\beta_2$ -GPI and added to the wells. After incubation and washing, ALP-conjugated streptavidin was used for detection. Assays were run triplicate. Error bars indicate SDs. K indicates kringle; mini-plg, mini-plasminogen.

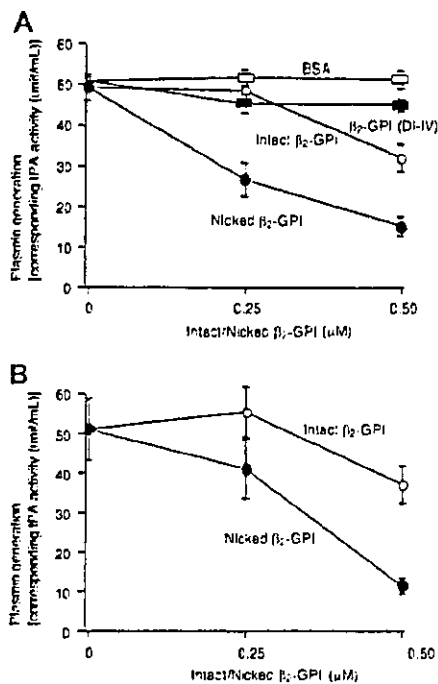


**Figure 6.** Inhibitory effect of nicked  $\beta_2$ -GPI on plasmin generation. (A) Plasmin generation was measured by parabolic rate assay using synthetic substrate S-2251 in the presence of tPA, Glu-plasminogen, and fibrin monomer. Nicked  $\beta_2$ -GPI ( $\bullet$ ), intact  $\beta_2$ -GPI ( $\circ$ ),  $\beta_2$ -GPI domain I-IV mutant ( $\blacksquare$ ), or BSA ( $\square$ ) was added to the reaction in the indicated concentrations. After 12 hours of incubation, absorbance at 405 nm was measured and expressed as tPA activity (U/mL) using tPA as standard. (B) Fibrinolytic activity was measured using fibrin plate assay. Solution reaction containing tPA, Glu-plasminogen, and nicked ( $\bullet$ ) or intact  $\beta_2$ -GPI ( $\circ$ ) were placed onto fibrin plates. After 36 hours of incubation, the ring area of lysis was measured. Assays were performed in triplicate. Error bars indicate SDs. D indicates domain.

phospholipid or plasminogen. The lysine-cluster patch in domain V of nicked  $\beta_2$ -GPI may gain accessibility for the LBS of Glu-plasminogen, whereas the C-terminal loop of intact  $\beta_2$ -GPI may

interfere with interactions of LBS and the Glu-plasminogen kringle 5.

The fibrinolytic system is regulated at different levels, either at plasminogen activation or at enzymatically active plasmin. Many factors, including  $\alpha_2$ -AP,  $\alpha_2$ -macroglobulin,  $\alpha_1$ -antitrypsin, inactivated C1, PAI-1, and PAI-2, prevent the overactivation of the fibrinolytic system. The most potent inhibitors are  $\alpha_2$ -AP and PAI-1<sup>37</sup>; the former binds to a component of kringle 1 to 3 of plasminogen<sup>38</sup> and can neutralize the generated plasmin more rapidly than  $\alpha_2$ -macroglobulin.

Fibrinolysis initiates on binding of kringle 5 of plasminogen to lysine residues on fibrin followed by the binding of kringle 1 to 3 of plasminogen to lysine residues on the cleaved fibrin.  $\alpha_2$ -AP does not bind to kringle 5 of plasminogen, hence, does not seem to affect the first interaction. Based on the observation that nicked  $\beta_2$ -GPI interferes the binding between Glu-plasminogen and fibrin monomer (Figure 5D), it is likely that the binding of nicked  $\beta_2$ -GPI to Glu-plasminogen affects the first step of fibrinolysis at least and exerts an inhibitory function in the fibrinolytic system via different mechanisms from that of  $\alpha_2$ -AP.

In conclusion, first we have demonstrated that plasma levels of nicked  $\beta_2$ -GPI can be a sensitive marker of cerebral ischemic events and we suggest that plasma measurement of nicked  $\beta_2$ -GPI might be a useful screening tool in the assessment of patients at risk of ischemic stroke. Second, we propose that nicked  $\beta_2$ -GPI is a physiologic inhibitor of fibrinolysis and that plasmin cleavage of  $\beta_2$ -GPI is part of the negative feedback pathway of extrinsic fibrinolysis.

## Acknowledgment

We wish to thank Professor Koji Suzuki, from Department of Molecular Pathobiology, Mie University School of Medicine, Tsu, Japan, for great suggestions and fruitful discussions.

## References

- Galli M, Comfurius P, Maassen C, et al. Anticardiolipin antibodies (ACA) directed not to cardiolipin but to a plasma protein cofactor. *Lancet*. 1990;335:1544-1547.
- McNeil HP, Simpson RJ, Chesterman CN, Krilis SA. Anti-phospholipid antibodies are directed against a complex antigen that induces a lipid-binding inhibitor of coagulation:  $\beta_2$ -glycoprotein I (apolipoprotein H). *Proc Natl Acad Sci U S A*. 1990;87:4120-4124.
- Matsuura E, Igarashi Y, Fujimoto M, Ichikawa K, Koike T. Anticardiolipin cofactor(s) and differential diagnosis of autoimmune disease. *Lancet*. 1990;336:177-178.
- Hughes GRV. The antiphospholipid syndrome: ten years on. *Lancet*. 1993;342:341-344.
- Hunt JE, Simpson RJ, Krilis SA. Identification of a region of  $\beta_2$ -glycoprotein I critical for lipid binding and anti-cardiolipin antibody cofactor activity. *Proc Natl Acad Sci U S A*. 1993;90:2141-2145.
- Ohkura N, Hagihara Y, Yoshimura T, Goto Y, Kato H. Plasmin can reduce the function of human  $\beta_2$  glycoprotein I by cleaving domain V into a nicked form. *Blood*. 1998;91:4173-4179.
- Nimpf J, Bevers EM, Bomans PHH, et al. Prothrombinase activity of human platelets inhibited by  $\beta_2$ -glycoprotein I. *Biochem Biophys Acta*. 1986;884:142-149.
- Shi W, Chong BH, Hogg PJ, Chesterman CN. Anticardiolipin antibodies block the inhibition by  $\beta_2$ -glycoprotein I of the factor Xa generating activity of platelets. *Thromb Haemost*. 1993;70:342-345.
- Schousboe I, Rasmussen MS. Synchronized inhibition of the phospholipid mediated autoactivation of factor XII in plasma by  $\beta_2$ -glycoprotein I and anti- $\beta_2$ -glycoprotein I. *Thromb Haemost*. 1995;73:798-804.
- Mori T, Takeya H, Nishioka J, Gabazza EC, Suzuki K.  $\beta_2$ -Glycoprotein I modulates the anticoagulant activity of activated protein C on the phospholipid surface. *Thromb Haemost*. 1996;75:49-55.
- Ieko M, Ichikawa K, Triplett DA, et al.  $\beta_2$ -Glycoprotein I is necessary to inhibit protein C activity by monoclonal anticardiolipin antibodies. *Arthritis Rheum*. 1999;42:167-174.
- Nakaya Y, Schaefer EJ, Brewer HBJ. Activation of human post heparin lipoprotein lipase by apolipoprotein H ( $\beta_2$ -glycoprotein I). *Biochem Biophys Res Commun*. 1980;95:1168-1172.
- Wurm H, Beubler E, Polz E, Holasek A, Kostner G. Studies on the possible function of  $\beta_2$ -glycoprotein-I: influence in the triglyceride metabolism in the rat. *Metabolism*. 1982;31:484-486.
- Hasunuma Y, Matsuura E, Makita Z, Katahira T, Nishi S, Koike T. Involvement of  $\beta_2$ -glycoprotein I and anticardiolipin antibodies in oxidatively modified low-density lipoprotein uptake by macrophages. *Clin Exp Immunol*. 1997;107:569-573.
- Chonn A, Semple SC, Cullis PR.  $\beta_2$  glycoprotein I is a major protein associated with very rapidly cleared liposomes in vivo, suggesting a significant role in the immune clearance of "non-self" particles. *J Biol Chem*. 1995;270:25845-25849.
- Manfredi AA, Rovere P, Galati G, et al. Apoptotic cell clearance in systemic lupus erythematosus: I: opsonization by antiphospholipid antibodies. *Arthritis Rheum*. 1998;41:205-214.
- Manfredi AA, Rovere P, Hellai S, et al. Apoptotic cell clearance in systemic lupus erythematosus: II: role of  $\beta_2$ -glycoprotein I. *Arthritis Rheum*. 1998;41:215-223.
- Wallen P, Wiman B. Characterization of human plasminogen: I. on the relationship between different molecular forms of plasminogen demonstrated in plasma and found in purified preparations. *Biochim Biophys Acta*. 1970;221:20-30.
- Ponting CP, Holland SK, Cederholm-Williams SA, et al. The compact domain conformation of human Glu-plasminogen in solution. *Biochim Biophys Acta*. 1992;1159:155-161.
- Aoki N, Saito H, Kamiya T, Koie K, Sakata Y, Kobakura M. Congenital deficiency of  $\alpha_2$ -plasmin inhibitor associated with severe hemorrhagic tendency. *J Clin Invest*. 1979;63:877-884.
- Loskutov DJ, Sawdey M, Mimuro J. Type 1 plasminogen activator inhibitor. *Frog Hemost Thromb*. 1989;9:87-115.
- Horbach DA, van Oort ET, Lisman T, Meijers JC.

- Derksen RH, de Groot PG.  $\beta$ 2-Glycoprotein I is proteolytically cleaved *in vivo* upon activation of fibrinolysis. *Thromb Haemost*. 1999;81:87-95.
23. Itoh Y, Inuzuka K, Kohno I, et al. Highly increased plasma concentrations of the nicked form of  $\beta$ 2-glycoprotein I in patients with leukemia and with lupus anticoagulant: measurement with a monoclonal antibody specific for a nicked form of domain V. *J Biochem (Tokyo)*. 2000;128:1017-1024.
  24. Igarashi M, Matsuura E, Igarashi Y, et al. Human  $\beta$ 2-glycoprotein I as an anticardiolipin cofactor determined using deleted mutants expressed by a Baculovirus system. *Blood*. 1996;87:3262-3270.
  25. Matsuura E, Igarashi Y, Fujimoto M, et al. Heterogeneity of anticardiolipin antibodies defined by the anticardiolipin cofactor. *J Immunol*. 1992;148:3885-3891.
  26. Matsuura E, Inagaki J, Kasahara H, et al. Proteolytic cleavage of  $\beta$ 2-glycoprotein I: reduction of antigenicity and the structural relationship. *Int Immunol*. 2000;12:1183-1192.
  27. Ranby M, Wallen P. A sensitive parabolic rate assay for tissue plasminogen activator. In: Davidson JF, Nilsson IM, Asted B, eds. *Progress in Fibrinolysis*. Vol 5. New York, NY: Churchill Livingstone; 1981:232-235.
  28. Bouma B, de Groot PG, van den Elsen JM, et al. Adhesion mechanism of human  $\beta$ 2-glycoprotein I to phospholipids based on its crystal structure. *EMBO J*. 1999;18:5166-5174.
  29. Schwarzenbacher R, Zeth K, Diederichs K, et al. Crystal structure of human  $\beta$ 2-glycoprotein I: implications for phospholipid binding and the antiphospholipid syndrome. *EMBO J*. 1999;18:6228-6239.
  30. Hoshino M, Hagihara Y, Nishii I, Yamazaki T, Kato H, Goto Y. Identification of the phospholipid-binding site of human  $\beta$ 2-glycoprotein I domain V by heteronuclear magnetic resonance. *J Mol Biol*. 2000;304:927-939.
  31. Lucas MA, Fretto LJ, McKee PA. The binding of human plasminogen to fibrin and fibrinogen. *J Biol Chem*. 1983;258:4249-4256.
  32. Wu HL, Chang BI, Wu DH, et al. Interaction of plasminogen and fibrin in plasminogen activation. *J Biol Chem*. 1990;265:19658-19664.
  33. Christensen U. C-terminal lysine residues of fibrinogen fragments essential for binding to plasminogen. *FEBS Lett*. 1985;182:43-46.
  34. Tran-Thang C, Kruihof EK, Atkinson J, Bachmann F. High-affinity binding sites for human Glu-plasminogen unveiled by limited plasmic degradation of human fibrin. *Eur J Biochem*. 1986;160:599-604.
  35. Matsuka YV, Novokhatny VV, Kudinov SA. Fluorescence spectroscopic analysis of ligand binding to kringle 1 + 2 + 3 and kringle 1 fragments from human plasminogen. *Eur J Biochem*. 1990;190:93-97.
  36. Chang Y, Mochalkin I, McCance SG, Cheng B, Tulinsky A, Castellino FJ. Structure and ligand binding determinants of the recombinant kringle 5 domain of human plasminogen. *Biochemistry*. 1998;37:3258-3271.
  37. Collen D, Lijnen HR. Basic and clinical aspects of fibrinolysis and thrombolysis. *Blood*. 1991;78:3114-3124.
  38. Thorsen S, Clemmensen I, Sottrup-Jensen L, Magnusson S. Adsorption to fibrin of native fragments of known primary structure from human plasminogen. *Biochem Biophys Acta*. 1981;668:377-387.

# The p38 mitogen-activated protein kinase (MAPK) pathway mediates induction of the tissue factor gene in monocytes stimulated with human monoclonal anti- $\beta_2$ Glycoprotein I antibodies

Miyuki Bohgaki, Tatsuya Atsumi, Yumi Yamashita, Shinsuke Yasuda, Yoshie Sakai, Akira Furusaki, Toshiyuki Bohgaki, Olga Amengual, Yoshiharu Amasaki and Takao Koike

Department of Medicine II, Hokkaido University Graduate School of Medicine, N-15 W-7, Kita-ku, Sapporo 060-8648, Japan

**Keywords:** anti-cardiolipin antibody, anti-phospholipid antibody, anti-phospholipid syndrome, thrombosis

## Abstract

The anti-phospholipid syndrome (APS) is characterized by thrombosis and the presence of anti-phospholipid antibodies (aPL). Tissue factor (TF), the major initiator of the coagulation system, is induced on monocytes by aPL *in vitro*, explaining, in part, the pathophysiology in this syndrome. However, little is known regarding the nature of the aPL-induced signal transduction pathways leading to TF expression. In this study, we investigated aPL-inducible genes in PBMC using cDNA array system and real-time PCR. Our results indicated that the mitogen-activated protein kinase (MAPK) pathway was related to TF expression when PBMCs were treated, in the presence of  $\beta_2$ Glycoprotein I ( $\beta_2$ GPI), with human monoclonal anti- $\beta_2$ GPI antibodies [ $\beta_2$ GPI-dependent anti-cardiolipin antibodies (aCL/ $\beta_2$ GPI)]. Western blotting studies using monocyte cell line (RAW264.7) demonstrated that p38 MAPK protein was phosphorylated with nuclear factor  $\kappa$ B (NF- $\kappa$ B) activation by monoclonal aCL/ $\beta_2$ GPI treatment, and that SB203580, a specific p38 MAPK inhibitor, decreased the aCL/ $\beta_2$ GPI-induced TF mRNA expression. The p38 MAPK phosphorylation, NF- $\kappa$ B translocation and TF mRNA expression triggered by aCL/ $\beta_2$ GPI were abolished in the absence of  $\beta_2$ GPI. These results demonstrated that the p38 MAPK signaling pathway plays an important role in aPL-induced TF expression on monocytes and suggest that the p38 MAPK may be a possible therapeutic target to modify a pro-thrombotic state in patients with APS.

## Introduction

Anti-phospholipid syndrome (APS) is a clinical condition characterized by recurrent thrombotic events and/or pregnancy morbidity associated with the persistence of anti-phospholipid antibodies (aPL) (1). Anti-cardiolipin antibodies (aCL) are members of the aPL family, a large and heterogeneous group of circulating Igs arising in a wide range of infectious and autoimmune diseases, particularly systemic lupus erythematosus (1). Since the early 1980s, the interest in aCL has exponentially increased due to their association with clinical manifestations of APS (2, 3).

aCL are detected by immunological assays (radioimmunoassay and ELISA) (2, 4, 5). Many studies have indicated that antibodies against  $\beta_2$ Glycoprotein I ( $\beta_2$ GPI) are one of the predominant antibodies detected with aCL assay in APS patients (6–12). APS-related aCL recognizes the epitope(s) on the

$\beta_2$ GPI molecule when  $\beta_2$ GPI interacts with a lipid membrane composed of negatively charged phospholipids [ $\beta_2$ GPI-dependent anti-cardiolipin antibodies or antibodies against cardiolipin/ $\beta_2$ GPI complex (aCL/ $\beta_2$ GPI)] (11). In the past decade, many studies have investigated the pathophysiology of thrombosis in APS and considerable interest has focused on the role of aPL as a clue to mechanisms related to thrombosis (13). Results of intensive research works have significantly advanced understanding of the mechanisms by which these antibodies may play a direct role in clot formation. Classically, *in vitro* evidence suggests that aCL/ $\beta_2$ GPI are involved in hemostatic abnormality.  $\beta_2$ GPI interacts with negatively charged phospholipids involved in the coagulation process, having both pro-coagulant and anticoagulant properties.  $\beta_2$ GPI suppresses the thrombomodulin–protein C system

Correspondence to: T. Atsumi; E-mail: at3tat@med.hokudai.ac.jp

Transmitting editor: K. Okumura

Received 11 August 2004, accepted 27 August 2004

(14), factor X, XI and XII activation (15–18) and pro-thrombinase activity (19). Antibodies against  $\beta_2$ GPI may modify the properties of  $\beta_2$ GPI and favor a pro-thrombotic state.

However, individuals with  $\beta_2$ GPI deficiency do not have a thrombotic tendency, thus aCL/ $\beta_2$ GPI-associated thrombosis cannot be merely explained by ' $\beta_2$ GPI insufficiency' (20, 21). Investigators turned their focus on functions of endothelial or other cells which might be modified by aPL. In this scenario,  $\beta_2$ GPI serves as a 'co-factor' to prepare receptors for auto-antibody binding to cells. In this case, irrespective of the functions of  $\beta_2$ GPI itself, auto-antibodies against  $\beta_2$ GPI may alter the bound-endothelium properties from 'anti-thrombotic' to 'pro-thrombotic', leading to the production of pro-coagulant substances such as tissue factor (TF) (22, 23), vascular cell adhesion molecule-1, intercellular adhesion molecule-1, E-selectin (24–26), plasminogen activator inhibitor-1 or endothelin-1 (27).

TF is the major initiator of the extrinsic coagulation system (28), functioning as the protein co-factor for the plasma serine protease, activated factor VII (FVIIa) (29, 30). Induced TF forms a complex with FVIIa that triggers the blood clotting cascade by activating factors IX and X, leading to thrombin generation (29). In normal conditions, TF is not expressed on intra-vascular cells (28) but it can be induced under stimuli such as LPS (31), tumor necrosis factor- $\alpha$  (TNF- $\alpha$ ) (32, 33) and IL-1 (34). Evidence has supported the role of TF pathway in the pathogenesis of aPL-related thrombosis (22, 23, 35–37). Preliminary experimental data showed that sera or IgG fraction containing aCL induce TF-like pro-coagulant activity in endothelial cell (38, 39) or PBMC (40, 41). We and others demonstrated the up-regulation of TF pathway in patients with APS (35, 42, 43). Patients with APS have a pro-thrombotic state as evidenced by elevated basal thrombin generation (37, 44). Increased TF expression on endothelial cell or monocytes induced by aPL could, in part, be responsible for the hyper-coagulability and explain the existence of thrombosis in both the arterial and venous circulation that characterizes those patients.

On the other hand, only a few data have been published regarding the intracellular pathway in aPL-induced expression of TF or other pro-coagulant substances. We screened gene expression of molecules involved in signal transmission in aCL/ $\beta_2$ GPI-induced TF expression using cDNA array system and demonstrated the significance of the p38 mitogen-activated protein kinase (MAPK) phosphorylation procedure in such cell activation.

## Methods

### *Isolation and preparation of cells*

Venous blood was collected in heparin from healthy donors. PBMCs were isolated on Ficoll-Paque plus<sup>®</sup> gradient centrifugation (Amersham Biosciences Corp., Piscataway, NJ, USA). PBMCs were washed with RPMI-1640 medium (Sigma Chemical Co., St Louis, MO, USA) supplemented with 10% FCS (GIBCO BRL, Paisley, UK) containing penicillin and streptomycin (RPMI-10 medium) once at 20°C, 400 × g, for 5 min and twice at 4°C, 400 × g, for 5 min. PBMCs were then

re-suspended in RPMI-10 medium and counted using the trypan blue dye exclusion method. Murine RAW264.7 (American Type Culture Collection registration no. #TIB-71) monocytes were maintained in a 5% CO<sub>2</sub> atmosphere at 37°C in DMEM (GIBCO BRL) supplemented with 10% FCS containing penicillin and streptomycin.

### *Proteins*

Human  $\beta_2$ GPI was purified from normal sera, as described (11), and the purity was confirmed using SDS-PAGE. Fatty acid-free BSA was obtained from Sigma-Aldrich Inc. (A-6002; St Louis, MO, USA). Two human IgM monoclonal aCL/ $\beta_2$ GPI (EY2C9 and TM1G2) and one control monoclonal IgM lacking aCL/ $\beta_2$ GPI activity (TM1B9) were used in this study. EY2C9 and TM1G2 are IgM class human monoclonal aCL/ $\beta_2$ GPI established from APS patients with high titers of aCL/ $\beta_2$ GPI (45). The characteristic of EY2C9 and TM1G2 is that these are mAbs that bind to the cardiolipin- $\beta_2$ GPI complex but not to cardiolipin alone (45). In the absence of cardiolipin, they do not recognize  $\beta_2$ GPI immobilized on the plain ELISA plate, but do bind to  $\beta_2$ GPI coated on an oxidized ELISA plate. The epitope mapping by phage-displayed peptide library demonstrated W<sup>235</sup> in the fourth domain of  $\beta_2$ GPI as a key amino acid residue at the epitopic center (46). Therefore, we consider that these mAbs represent autoimmune aCL/ $\beta_2$ GPI found in patients with APS. The mAbs, when purified from serum-free medium culture supernatant, showed a single band on SDS-PAGE. LPS were intensively removed from these antibody preparations with DetoxiGel<sup>®</sup> (Pierce, Rockford, IL, USA) and were not detected using the *Limulus* amoebocyte lysate assay (Limulus ES-II Single Test Wako: Wako, Osaka, Japan).

### *RNA extraction and cDNA array analysis*

Total RNAs were isolated from PBMC or RAW264.7 using TRIzol<sup>®</sup> reagent (Invitrogen, Carlsbad, CA, USA), and stored at –80°C until use. Poly(A) RNA was isolated from total RNA (100  $\mu$ g) using a MagExtractor<sup>®</sup> (TOYOBO, Osaka, Japan), and poly(A) RNA (2  $\mu$ g) was reverse transcribed by ReverTraAce (TOYOBO) in the presence of cDNA synthesis primers and biotin-16-deoxyuridine triphosphate (TOYOBO), according to the manufacturer's instructions. cDNA array analysis was performed using human cDNA expression filters [Human Immunology Filters (TOYOBO), on which 621 species of human cDNA fragments and housekeeping genes were duplicated spotted]. Genes on the filter are shown on the web site <http://www.toyobo.co.jp/seihin/xr/product/genenavi/genenavigator.html>. Hybridization and subsequent cDNA array analyses were done as described (47), but with some modification. Briefly, cDNA array filters were pre-hybridized with PerfectHyb<sup>®</sup> solution (TOYOBO), and then hybridized with a biotin-labeled cDNA probe overnight at 68°C. After washing under high-stringency conditions, specific signals on the filters were visualized using Phototope-Star Detection Kits (New England Biolabs, Beverly, MA, USA), according to the manufacturer's recommendation. Fluorescence signals for mRNA expression levels were obtained using a Fluor-S Multiimager system (Nippon Bio-Rad Laboratories, Tokyo, Japan) and intensity of the signals was determined using ImaGene 4.2 software (BioDiscovery, Los Angeles, CA, USA).

Glyceraldehyde-3-phosphate dehydrogenase (GAPDH) mRNA was used as an internal control to normalize the mRNA abundance. The signal intensity among filters was compared in an E-Gene Navigator Analysis (GeneticLab, Sapporo, Japan) and expressed as mRNA expression index to the intensity of the internal GAPDH gene.

#### Quantitative TaqMan real-time PCR

Real-time PCR amplification and determination were done using the ABI PRISM 7000<sup>®</sup> Sequence Detection System (Applied Biosystems, Foster City, CA, USA) and gene-specific sets of TaqMan Universal PCR Master Mix<sup>®</sup> and Assays-on-Demand<sup>®</sup> Gene Expression probes (Applied Biosystems). A standard curve for serial dilutions of GAPDH was generated using a standard method provided by the manufacturer (Applied Biosystems), and was used to determine the amounts of cDNA transcripts.

#### Western blot analyses

For western blot analysis of p38 phosphorylation and nuclear nuclear factor  $\kappa$ B (NF- $\kappa$ B) translocation, PBMC or RAW264.7 cells were treated with monoclonal aCL/ $\beta_2$ GPI (10  $\mu$ g ml<sup>-1</sup>) or control mAb in the presence/absence of  $\beta_2$ GPI (50  $\mu$ g ml<sup>-1</sup>) in serum-free medium, or 10% FCS medium at 37°C, followed by a preparation of cytosolic and nuclear proteins using a proteome extraction kit (Merck, Darmstadt, Germany). The cell lysates were resolved on 10% SDS-PAGE gel and then transferred to polyvinylidene fluoride membranes (Millipore, Billerica, MA, USA). The membranes were blocked with PBS containing 5% non-fat dry milk (Nestle USA, Inc., Solon, OH, USA) and 0.1% Tween-PBS buffer for 1 h, and probed with the rabbit polyclonal anti-phospho-MAPK antibody using a Phospho-MAPK family antibody sampler kit (Cell Signaling Technology, Inc., Beverly, MA, USA) overnight at 4°C. For some experiments, the blots were stripped and re-probed with polyclonal anti-MAPK antibody that recognizes both activated and non-activated MAPK proteins using an MAPK family antibody sampler kit (Cell Signaling Technology, Inc.). After three washes in 0.1% Tween-PBS buffer, the membranes were exposed to HRP-conjugated goat anti-rabbit antibodies at room temperature. Immunoreactive proteins were visualized using enhanced chemiluminescence assay (Amersham Biosciences Corp.). For analysis of NF- $\kappa$ B, nuclear lysates from the stimulated cells were blotted and reacted with an anti-NF- $\kappa$ B antibody (Santa Cruz Biotechnology, Inc., Santa Cruz, CA, USA), the NF- $\kappa$ B antigen was visualized in the same fashion. In some experiments, the p38 MAPK inhibitor, SB203580 (Calbiochem, La Jolla, CA, USA), and the negative control for p38 MAPK inhibition studies, SB202474 (Calbiochem), were dissolved in dimethyl sulfoxide before addition to the culture medium.

#### Surface staining for FACS analysis

Surface aCL/ $\beta_2$ GPI binding on RAW264.7 was analyzed using FACSCalibur (Becton Dickinson Immunocytometry Systems, San Jose, CA, USA) with the CellQuest program. The cultured cells were washed with FACS buffer (2% BSA, 0.1% NaN<sub>3</sub> and PBS), and treated with 50  $\mu$ g ml<sup>-1</sup> of  $\beta_2$ GPI at room temperature for 10 min, followed by exposure to EY2C9 or TM1G2 (final concentration, 20  $\mu$ g ml<sup>-1</sup>) for 30 min on ice. After washing twice with FACS buffer, cells were stained with FITC-

conjugated goat anti-human IgG/IgM antibody (Jackson ImmunoResearch Laboratories, Inc., West Grove, PA, USA) for 30 min on ice. After further two washes with FACS buffer, cells were subjected to FACS analysis. For each sample, data from 10 000 volume-gated viable cells were collected.

## Results

#### Identification of monoclonal aCL/ $\beta_2$ GPI antibody-inducible genes

The effect of monoclonal aCL/ $\beta_2$ GPI on PBMC was screened utilizing cDNA arrays and mRNA expression of genes associated with the human immune system, including transcription factors, effector molecules and cytokines shown in Fig. 1. As a whole, the most increased mRNA expression by aCL/ $\beta_2$ GPI treatment in cell signaling was detected in 2-h incubated cells (Fig. 1A). In the 2-h cDNA array analysis in PBMC exposed to EY2C9 and control IgM, mRNA related to MAPK pathway such as p38 regulated/activated protein kinase, TNF receptor-associated factor 6 (TRAF6), Sp-1, SAPK4 (p38 $\delta$ ) and MAPK-activated protein kinase (MAPKAPK)-3 increased >2-fold in EY2C9-treated cells compared with those treated with control IgM (Fig. 1A and Fig. 1B, left). In contrast, the expression of other signaling pathway molecules (Fig. 1B, right), such as tyrosine kinase, protein kinase C and Akt kinases, increased <2-fold. The expression of pro-inflammatory cytokine genes such as TNF- $\alpha$  and IL-1 $\beta$ , known to be regulated by the MAPK pathway, were enhanced up to 2- to 4-fold in the cDNA array (Fig. 1C). To confirm the results of cDNA array screening and previously reported TF mRNA expression by stimulation of aCL/ $\beta_2$ GPI, a real-time PCR method was applied. Both EY2C9 and TM1G2 stimulation increased TF (Fig. 2A), TNF- $\alpha$  (Fig. 2B) and IL-1 $\beta$  (Fig. 2C) mRNA expression. Up-regulated TF mRNA expression was also detected using real-time PCR in the monocyte cell line RAW264.7 after treatment with EY2C9 or TM1G2 (data not shown).

#### Identification of p38 MAPK phosphorylation as a pathway of aCL/ $\beta_2$ GPI activation

According to the results of cDNA array analysis, some MAPK-related molecules were up-regulated in PBMC by stimulation with aCL/ $\beta_2$ GPI, therefore, we further asked if the cDNA array results were associated with MAPK pathway activation. Non-phosphorylated forms of MAPKs (total MAPKs) were detected in unstimulated RAW264.7 cells. Cells treated with EY2C9 showed phosphorylation of p38 MAPK, which persisted for at least 60 min (Fig. 3). In contrast with ERK and JNK phosphorylation by LPS, neither ERK nor JNK pathway was activated with EY2C9 stimulation (Fig. 3).

#### Reduction of p38 MAPK activation in aCL/ $\beta_2$ GPI-mediated up-regulation of TF expression

To elucidate the role of p38 MAPK in TF mRNA expression, the effect of p38 MAPK inhibitors on the cells stimulated with monoclonal aCL/ $\beta_2$ GPI was examined. The p38-specific inhibitor, SB203580, entirely hampered p38 MAPK phosphorylation in RAW264.7 treated with EY2C9 (Fig. 4A), but SB202474, the inactive analogue of SB203580, did not affect



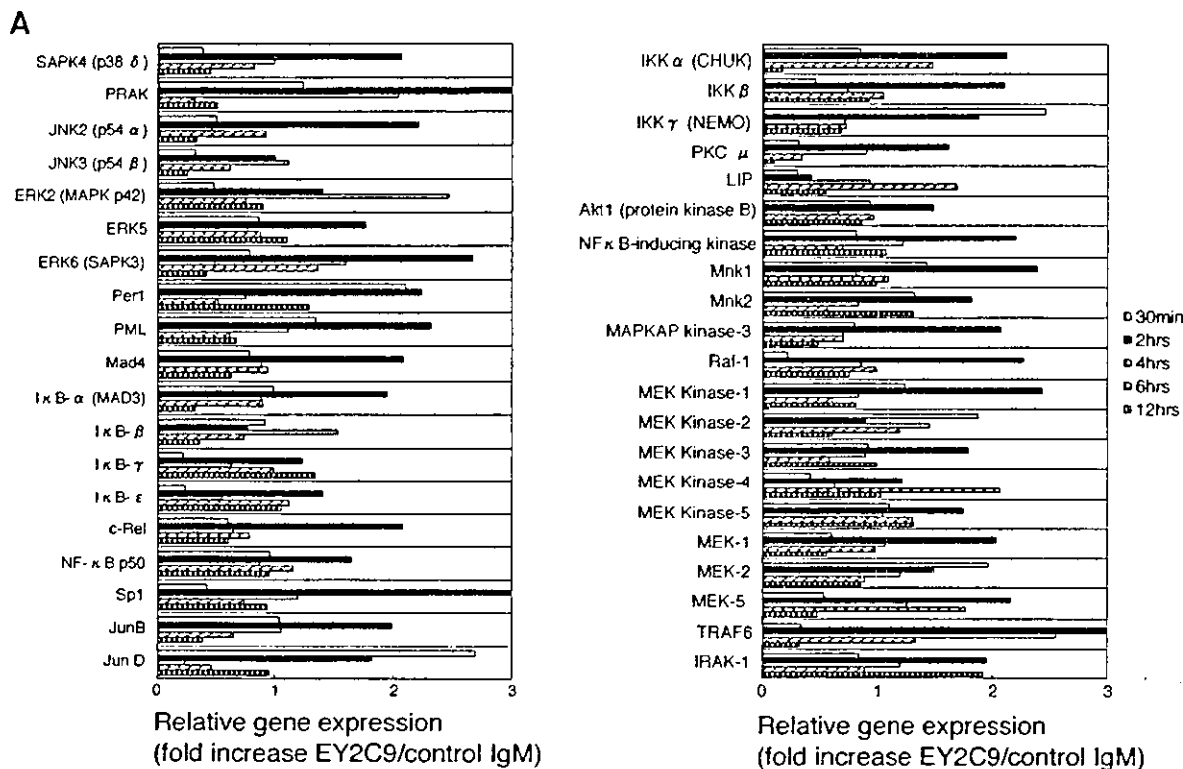


**Fig. 1.** Screening of up-regulated genes induced by monoclonal aCL/ $\beta_2$ GPI in PBMC: mRNA level of genes encoding various intracellular signaling transcription factors and molecules. PBMCs were stimulated with monoclonal IgM aCL/ $\beta_2$ GPI (EY2C9) or control antibody at  $30 \mu\text{g ml}^{-1}$  for 30 min and 2, 4, 6 and 12 h. mRNA expression levels were analyzed by cDNA array as described in Methods. A. mRNA expression level of selected genes encoding mainly those associated with the MAPK pathway. These panels show fold increases in the mRNA expression level in EY2C9-stimulated cells compared with that in control IgM-stimulated cells. Increased mRNA expression was detected in 2-h incubated cells. B. Two-hour cDNA array analysis. mRNA expression level of selected genes encoding mainly those associated with the MAPK pathway (left panel) and various other signaling pathways (right panel). Genes are put in order of mRNA expression levels in each panel. PBMCs were treated with monoclonal IgM aCL/ $\beta_2$ GPI (EY2C9) or control antibody at  $30 \mu\text{g ml}^{-1}$  for 2 h. mRNA expression levels were analyzed using cDNA array as described in Methods, and shows fold increase of the mRNA expression level in EY2C9-stimulated cells compared with that in control IgM-stimulated cells. MAPK-related molecule mRNA expressions are higher than other cell signal transduction molecules. C. mRNA expression level of some selected genes encoding cytokines and chemokines. This panel shows fold increases in the mRNA expression level in EY2C9-stimulated cells for 2 h compared with that in control IgM-stimulated cells for 2 h.

p38 phosphorylation. Addition of SB203580 to cells stimulated with EY2C9 or TM1G2 decreased TF mRNA expression up to 75% (Fig. 4B).

#### $\beta_2$ GPI dependency of p38 MAPK phosphorylation and TF induction

To evaluate the  $\beta_2$ GPI dependency of EY2C9 stimulation, we established RAW264.7 cells adapted to serum-free medium and treated these cells with EY2C9 in the absence/presence of human  $\beta_2$ GPI. In the cells stimulated by EY2C9, p38 MAPK phosphorylation was observed in the presence of  $\beta_2$ GPI either in serum-free medium or in medium supplemented with 10% FCS, but there was no apparent effect of this monoclonal aCL/ $\beta_2$ GPI in the absence of  $\beta_2$ GPI (Fig. 5A). In addition, NF- $\kappa$ B was increased in the nuclear fraction after stimulation with EY2C9 in the presence of  $\beta_2$ GPI (Fig. 5A). Furthermore, EY2C9 or TM1G2 induced RAW264.7 TF mRNA expression in a  $\beta_2$ GPI-dependent manner, whereas  $\beta_2$ GPI had little effect on LPS-induced expression of TF mRNA (Fig. 5B). In FACS analysis, EY2C9 bound to the cells in the presence of  $\beta_2$ GPI, but no binding of EY2C9 was found in the absence of  $\beta_2$ GPI (data not shown).

#### Discussion

In the present study, we demonstrated that the p38 MAPK-dependent signaling pathway participates in aPL-mediated TF expression. The multi-screening using the cDNA array system combined with real-time PCR analysis indicated that the MAPK pathway was related to TF expression when cells were treated with monoclonal aCL/ $\beta_2$ GPI. We performed western blotting studies to confirm the result of cDNA array at protein level that p38 MAPK protein was phosphorylated. The specific p38 MAPK inhibitor decreased TF mRNA expression by aCL/ $\beta_2$ GPI stimulation, suggesting a crucial role of the p38 MAPK pathway in this system.

The association between aPL and the occurrence of thrombosis is widely recognized. The effect of aCL in the inhibition of natural anticoagulant systems, the impairment of fibrinolytic activity and the direct effect of these antibodies on cell functions or injury are some of the proposed mechanisms to explain the thrombotic tendency of patients with APS. Endothelial cells, monocytes and activated platelets may be a predominant target of aCL/ $\beta_2$ GPI associated with the pro-coagulant state characteristic of APS.

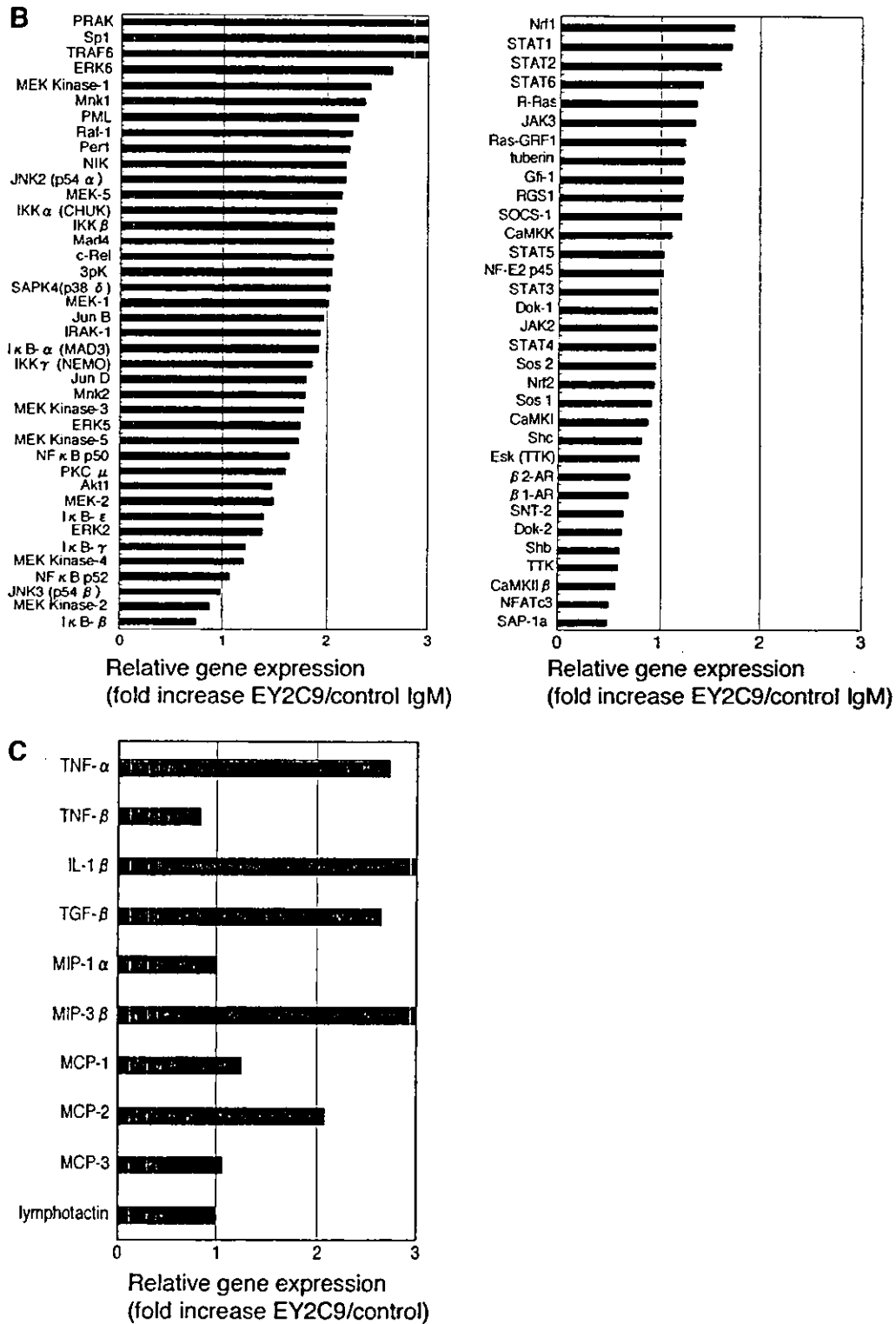
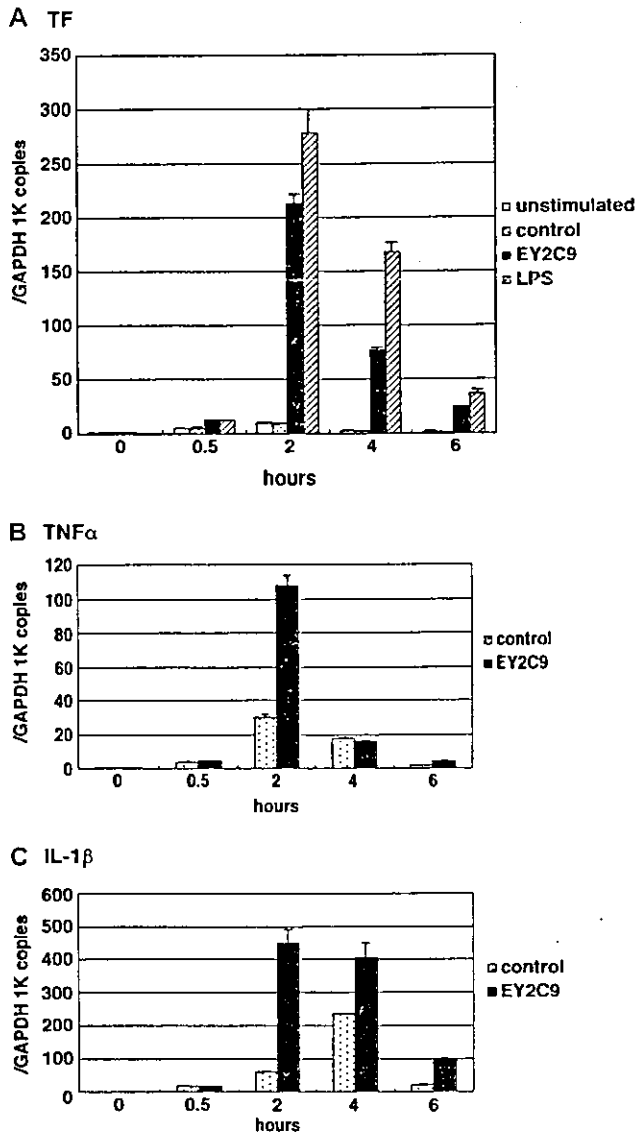


Fig. 1. Continued.

Pro-coagulant cell activation, accompanied with TF expression and TF pathway up-regulation, is one of the key events considered to explain the pathophysiology of thrombosis in

patients with APS. We showed elevated plasma levels of soluble TF in APS patients (22, 35), and Cuadrado *et al.* (42) reported that monocytes prepared from APS patients had high



**Fig. 2.** Expression of TF, TNF- $\alpha$  and IL-1 $\beta$  mRNA in PBMCs treated with monoclonal aCL/ $\beta_2$ GPI. PBMCs were stimulated with 10  $\mu$ g ml<sup>-1</sup> monoclonal IgM aCL/ $\beta_2$ GPI (EY2C9 or TM1G2) or control IgM antibody (TM1B9) for 30 min and 2, 4 and 6 h. mRNA expression of TF (A), TNF- $\alpha$  (B) and IL-1 $\beta$  (C) were analyzed using real-time PCR as described in Methods. The maximum increase was observed at 2 h stimulation. Each column represents the average  $\pm$  SD of three independent experiments.

TF expression. Tissue factor pathway inhibitor (TFPI), a physiological inhibitor of the extrinsic coagulation system, was also increased in plasma from patients with APS (22), suggesting up-regulation of TF and TFPI in affected patients. In *in vitro* experiments, numerous reports show that the IgG fraction from patients with aPL induced pro-coagulant activity on cells (38–41, 48). Our previous observation that human monoclonal aCL/ $\beta_2$ GPI induced TF mRNA and TF activity on PBMC and endothelium was confirmed by Reverter *et al.* (23) using the same mAbs. Apart from the TF molecule, other pro-coagulant substances induced by aPL were extensively investigated. Del

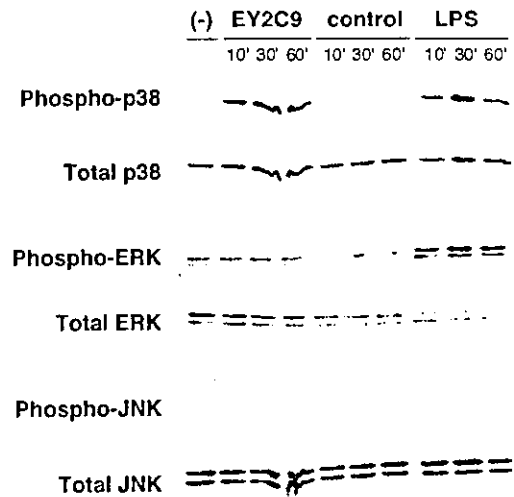


**Fig. 3.** MAPK phosphorylation in response to EY2C9. Mouse monocyte cell line RAW264.7 cells were stimulated with EY2C9 or control IgM antibody (TM1B9) for 10, 30 and 60 min. MAPK activation was determined by western blot using specific antibodies against total-p38, -ERK and -JNK/SAPK, and phospho-p38, -ERK and -JNK/SAPK.

Papa *et al.* (24, 49–51) have reported a series of molecules associated with endothelium activation by aPL *in vitro*, and other groups (25, 26) have shown adhesion molecules expression induced by IgG with aPL activity *in vitro* and *in vivo* models. Thus, it is widely accepted that aPL can induce the expression of TF or other pro-coagulant substances on cells in some conditions.

Recently, the signal transduction mechanism has been explored and associated with the increased expression of pro-coagulant substances in response to aPL. Dunoyer-Geindre *et al.* (52) presented an indirect but essential role of NF- $\kappa$ B in endothelial cell activation by aPL. IgG purified from APS patients induced the nuclear translocation of NF- $\kappa$ B leading to the transcription of a large number of genes that have a NF- $\kappa$ B-responsive element in their promoter. This nuclear translocation of NF- $\kappa$ B, at least in part, can explain the increased expression of TF by endothelial cell.

Protein kinases are key regulators of cellular signaling that control inflammation, cell differentiation, cell growth and cell death, and thus have been attractive targets for the treatment of neoplasms and inflammatory diseases. p38 MAPK was originally identified as a target molecule for a protein kinase inhibitor SB203580, a pyridinyl imidazole derivative which inhibits the production of pro-inflammatory cytokines. Isoforms of p38 MAPK are strongly activated by environmental stress or inflammatory cytokines [for review, see ref. (53)]. MAPK/ERK kinase (MEK)3 and MEK6, MAPKKs which obtain high specificity for p38, are activated by several MAPKKKs that become active by oxidative stress, ultraviolet irradiation, hypoxia, ischemia, Gram-negative bacteria-derived LPS (54, 55) or inflammatory cytokines such as TNF- $\alpha$ , IL-1 $\beta$  and IL-18. Accordingly, activation of p38 is considered to be critical for normal immune responses, and properties of the p38 pathway in inflammatory process have been investigated.

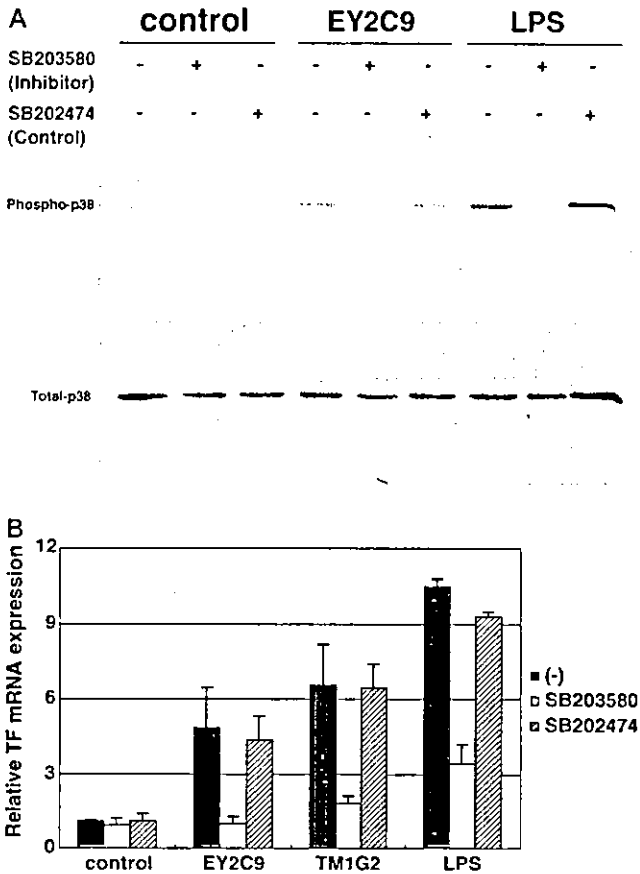


**Fig. 4.** Effect of p38 inhibitor on response to monoclonal IgM aCL/ $\beta_2$ GPI. **A.** RAW264.7 cells were treated with EY2C9 or control IgM antibody, in the presence or absence of SB203580 (200 nM) or SB202474 (200 nM) for 30 min. The phosphorylation of p38 was determined by western blotting. **B.** RAW264.7 cells were treated with EY2C9 or TM1G2 or control IgM antibody, in the presence or absence of SB203580 (200 nM) or SB202474 (200 nM) for 4 h. TF mRNA levels were determined using real-time PCR and demonstrated fold increase of stimulated/unstimulated cells. Each column represents the average  $\pm$  SD of three independent experiments.

Activation of p38 MAPK increases activities of pro-inflammatory cytokines, such as TNF- $\alpha$  and IL-1 $\beta$ . Up-regulation of TNF- $\alpha$ , IL-1 $\beta$  and macrophage inflammatory protein 3 $\beta$  (MIP3 $\beta$ ) was also found in the present study (Figs 1C and 2B and C). Downstream of activated p38 MAPK, MAPKAPK-2/3 is a substrate for p38 that undergoes post-transcriptional regulation of TNF- $\alpha$ . p38 also activates transcriptional factors such as activating transcriptional factor-2, which forms a heterodimer with JUN family transcriptional factors and associates with the activator protein-1 (AP-1)-binding site. After LPS stimulation of dendritic cells, NH<sub>2</sub>-termini of histone H3 undergo structural alteration in a p38-dependent pathway, which results in enhancement of accessibility of the cryptic NF- $\kappa$ B-binding sites (56). The promoter region of the TF gene contains two AP-1-binding sites and one NF- $\kappa$ B-binding site, and these transcription factors are proven required for maximal induction of TF gene transcription. Moreover, p38 MAPK pathway has been implicated in the regulation of TF expression in monocytes, endothelial cells and smooth muscle cells (57–61).

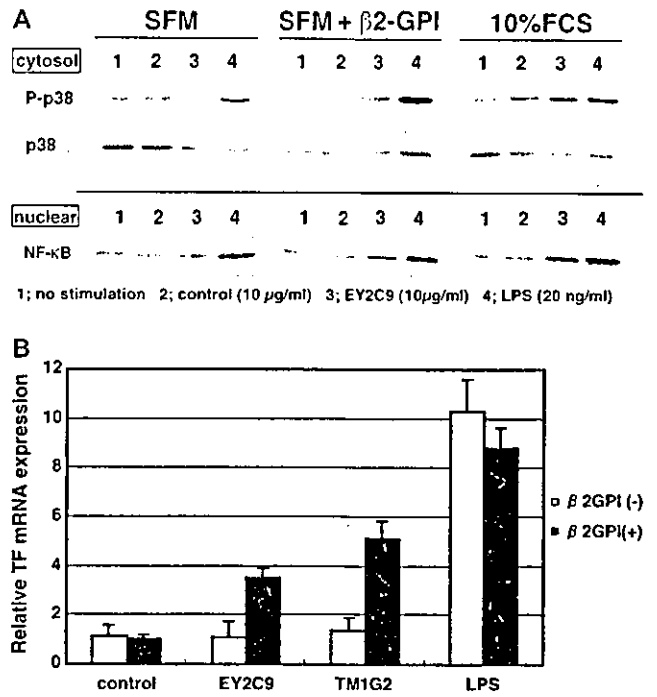


**Fig. 5.**  $\beta_2$ GPI dependency of monoclonal aCL/ $\beta_2$ GPI stimulation. **A.** Serum-free medium-adapted RAW264.7 were treated with EY2C9 or control IgM antibody, in the absence/presence of  $\beta_2$ GPI (50  $\mu$ g ml<sup>-1</sup>) or FCS (10%) for 30 min. The phosphorylation of p38 and nuclear/cytoplasmic localization of NF- $\kappa$ B were determined by western blotting. 1, no stimulation. 2, control (10  $\mu$ g ml<sup>-1</sup>). 3, EY2C9 (10  $\mu$ g ml<sup>-1</sup>). 4, LPS (20 ng ml<sup>-1</sup>). **B.** RAW264.7 were treated with EY2C9, TM1G2 or control IgM antibody, in the absence/presence of  $\beta_2$ GPI (50  $\mu$ g ml<sup>-1</sup>) or FCS (10%) for 4 h. TF mRNA levels were determined using real-time PCR and demonstrated fold increase of stimulated/unstimulated cells. Each column represents the average  $\pm$  SD of three separate experiments.

In the present study, we have shown that stimulation by monoclonal aCL/ $\beta_2$ GPI induced phosphorylation of p38, locational shift of NF- $\kappa$ B into the nucleus and up-regulation in TF expression. TF expression induced by aCL/ $\beta_2$ GPI occurred only in the presence of  $\beta_2$ GPI, suggesting that perturbation of monocytes by aCL/ $\beta_2$ GPI is initiated by interaction between the cell and the auto-antibody-bound  $\beta_2$ GPI. It remains to be determined how aCL/ $\beta_2$ GPI bind  $\beta_2$ GPI on the cell surface and how signal transduction events occur upstream of p38. Using endothelial cells, Raschi *et al.* (62) reported that the dominant negative construct of TRAF6 and that of myeloid differentiation protein 88 (MyD88) abrogated the NF- $\kappa$ B activation induced by monoclonal aCL/ $\beta_2$ GPI as well as that induced by IL-1 or LPS. They proposed that aCL/ $\beta_2$ GPI react with  $\beta_2$ GPI likely associated to a member of the Toll-like receptor (TLR)/IL-1 receptor family. The results of our study are compatible with this report; firstly, in our cDNA array experiment, the expression levels of the members of the MyD88 signaling pathway such as interleukin-1 receptor associated kinase 1 (IRAK-1), TRAF6 and I $\kappa$ B kinase  $\alpha$ ,  $\beta$  and  $\gamma$  were up-regulated after treatment with monoclonal aCL/ $\beta_2$ GPI (Fig. 1) and, secondly, TRAF6 activates MEK3 and MEK6 which are the kinases upstream of p38 and JNK via activation of an MAPKKK called transforming growth factor- $\beta$ -activated kinase. The different